Gas Turbines Fired on Coal Derived Gases – Modelling of Particulate and Vapour Deposition

Report No.
COAL R280
DTI/Pub
URN 05/661

March 2005

by

J E Fackrell, R J Tabberer, J B Young (Cambridge) and Z Wu (Cambridge)

E.ON UK (formerly Powergen UK)
Power Technology Centre
Ratcliffe-on-Soar
Nottingham
NG11 0EE

Tel: 0115 936 2502
Email: John.Fackrell@eon-uk.com

The work described in this report was carried out under contract as part of the DTI Cleaner Coal Research and Development Programme. The programme is managed by Mott MacDonald Ltd. The views and judgements expressed in this report are those of the contractor and do not necessarily reflect those of the DTI or Mott MacDonald Ltd

First published 2005

Final Report

Part 1

ALKALI SALT VAPOUR DEPOSITION ON GAS TURBINE BLADES

J.B. Young

Hopkinson Laboratory
Cambridge University Engineering Department

J.E.Fackrell and R. Tabberer

Powergen
Power Technology Centre
Ratcliffe-on-Soar

PRELIMINARY REMARKS

The following report describes the development of a computer program for calculating deposition rates of alakali salts from two-dimensional turbulent boundary layer flows on turbine blades. The description of the program was originally submitted as the Milestone 1 Report of the project. This description is included here, but with additional sections summarising the background and theoretical approach of the work and the application of the code to an example cleaner-coal turbine.

An alkali salt deposition code was originally developed during an earlier DTI supported cleaner-coal project (the Grimethorpe Topping Cycle Project), but this was written specifically for high chlorine UK coals. The present code is a development of that code to generalise it for use with world coals, which generally have lower chlorine levels. The opportunity was also taken to rewrite the code in Fortran 95 rather than the older Fortran 77 used for the original code.

The development and testing of the new code involved:

(i) Conducting a literature search for thermochemical data on the alkali oxide/hydroxide system;
(ii) Deriving appropriate thermochemical constants and parameters;
(iii) Revising the existing models to incorporate the alkali oxides and hydroxides;
(iv) Incorporating the new model into a computer program to estimate the boundary layer diffusion and surface deposition rates of the alkali salts;
(v) Performing sample test calculations with the new computer program.

Items (i), (ii) and (iii) were carried out by Mr. R. Tabberer of Powergen, item (iv) by Prof. J.B.Young of Cambridge University and item (v) by Dr. J.E. Fackrell of Powergen.

Dissemination of the results of this work will be via publication in technical journals (probably the *International Journal of Heat and Mass Transfer*) and it is planned to prepare and submit at least one journal paper by the end of 2004. The work will also be presented at specialist conferences.

There is considerable potential for exploitation of the existing computer code. As it stands, the code should be of interest to those companies involved in the design and manufacture of the type of heavy-duty industrial gas turbine which will be required in the future for coal-fired operation. The main companies operating worldwide are General Electric in the United States, Alstom in the United Kingdom, Siemens in Europe, and Mitsubishi and Hitachi in Japan. The Whittle Laboratory at Cambridge University has close contact with most of these (and other) companies and it is proposed to investigate the possibilities for marketing of the code and establishing other consulting arrangements.

There is also potential for further scientific development of the thermochemical modelling. Although attention has been confined in the present project to the salts of sodium and potassium and their behaviour in high temperature gas flows, the method of analysis is fairly general and could be extended to encompass other situations. For example, two problems of current interest which might respond to similar modelling techniques are the transport of corrosive vanadium salts to gas turbine blades in conventional gas turbines and corrosion of steam turbine blades by sodium salts present in the feedwater. In the United Kingdom, companies such as Rolls-Royce, Alstom and Siemens will be approached for discussion on the possibility of extending the modelling to deal with these and other technical problems.

1 INTRODUCTION

Many cleaner coal technologies, including various IGCC (Integrated Gasification Combined Cycle) and ABGC (Air Blown Gasification Cycle) technologies derive their high efficiency by coupling a gasification process with a gas turbine combined cycle unit. The coal is converted into a fuel gas which is then used to fire the combined cycle unit. Gas turbines are designed to operate on clean fuels such as natural gas whereas the fuel gas derived from coal will contain various impurities including alkali salts. These can cause deposits on the turbine blades resulting in corrosion. Conventional IGCC's can clean the fuel gas to high purity using low temperature processes. The ABGC and second generation IGCC's will use hot gas clean-up where the degree of alkali removal may not be as efficient. This will improve the efficiency of the plant and lower capital costs but may have deleterious effects on the gas turbine.

To predict the degree of corrosion in the gas turbine, it is necessary to model the deposition rate of alkali salts onto the turbine blades. A model for alkali salt vapour deposition was developed a few years ago during the Grimethorpe Topping Cycle Project and was successfully applied to predict corrosion for the Grimethorpe data. This model assumed that the alkali metals (sodium and potassium) were present in the gas phase as chloride salts (NaCl, KCl). This assumption was valid for the Grimethorpe modelling where a UK coal was being used which resulted in the formation of significant amounts of hydrogen chloride HCl in the fuel gas. More generally, for operation with world coals, the chloride levels are expected to be much lower and the principal alkali salt species present are likely to be the hydroxides (NaOH, KOH) and the oxides, particularly the superoxides (NaO_2, KO_2).

All coals contain sulphur and this gives rise to the presence of sulphur dioxide SO_2 at combustor outlet. The possibility therefore exists for the formation of the sulphates (Na_2SO_4, K_2SO_4). Calculations show, however, that at the high gas temperatures in the first stage of the turbine, equilibrium favours the chlorides, hydroxides and superoxides rather than the sulphates. Nevertheless, as these species diffuse through the turbulent boundary layers towards the blade surfaces, the temperature drops dramatically (because the blades are cooled) and the gas-phase equilibrium shifts in favour of the sulphates. The thermochemistry then predicts that, for most practical situations, the liquid or solid deposit which forms on the blade surface is composed almost entirely of the sulphates. This is true even when chlorine is present in the coal.

The present project involved reconfiguring the thermochemistry model and computer program to account for the presence of the oxides and hydroxides. The computer code is called VAPOURDEP and the user manual is appended.

2 OUTLINE OF THE THEORY

2.1 Equilibrium in the freestream

At combustor outlet, the particular species of interest present in the gas phase are :

$$O_2, \quad H_2O, \quad SO_2, \quad HCl.$$

It is assumed that the mole fractions of these species are fixed and known. O_2 and H_2O will be present in substantial quantities (mole fractions of order 10^{-1}) but the concentrations of SO_2 and HCl will be much less (mole fractions of order 10^{-4}). HCl will only be present if the original coal contained chlorine as well as sulphur.

There will also be trace amounts of sodium Na and potassium K present (typically mole fractions of order 10^{-8}). It is assumed that the total amounts of Na and K are known from an analysis of the original coal. A study of the Gibbs free enthalpy of formation of a range of possible sodium and potassium salts indicates that the most likely species to be present are :

$$NaCl, \quad NaOH, \quad NaO_2, \quad Na_2SO_4, \quad KCl, \quad KOH, \quad KO_2, \quad K_2SO_4.$$

At combustor outlet (turbine inlet) it is assumed that all species are in chemical equilibrium. The relevant equilibrium equations are:

$$\tfrac{1}{2}H_2O + \tfrac{1}{4}O_2 \leftrightarrow OH$$

$$NaO_2 + OH \leftrightarrow NaOH + O_2$$

$$KO_2 + OH \leftrightarrow KOH + O_2$$

$$2NaO_2 + SO_2 \leftrightarrow Na_2SO_4 + O_2$$

$$2KO_2 + SO_2 \leftrightarrow K_2SO_4 + O_2$$

$$2NaCl + H_2O + SO_2 + \tfrac{1}{2}O_2 \leftrightarrow Na_2SO_4 + 2HCl$$

$$2KCl + H_2O + SO_2 + \tfrac{1}{2}O_2 \leftrightarrow K_2SO_4 + 2HCl$$

These give rise to seven algebraic equations involving the seven corresponding equilibrium constants. There are also two equations for the known total amounts of Na and K. These nine equations are sufficient to solve for the nine unknown mole fractions of the species

$$NaCl, \quad NaOH, \quad NaO_2, \quad Na_2SO_4, \quad KCl, \quad KOH, \quad KO_2, \quad K_2SO_4, \quad OH,$$

at the given temperature and mixture pressure. Details of the equations and the method of solution is given in Appendix 1 of the attached computer program manual.

Between the combustor outlet and the mainstream flow in the turbine blade passage of interest, the temperature and pressure will change and the equilibrium between the nine

species may shift. Consideration of the rates of the various reactions suggests two possibilities, both of which are available as options within the computer program :

1) Full equilibrium prevails in the freestream of the turbine blade passage. In this case, the analysis is identical to that performed at combustor outlet but is carried out at the local pressure and temperature of interest.

2) The mole fractions of Na_2SO_4 and K_2SO_4 are assumed frozen at the combustor outlet value but all other species maintain their equilibrium concentrations. This is considered the more realistic possibility because the formation of Na_2SO_4 and K_2SO_4 each requires the collision of two sodium or potassium species which, given the extremely low concentrations, must be a comparatively rare event. The analysis for frozen Na_2SO_4 and K_2SO_4 is similar to the full equilibrium calculation but only five (rather than seven) chemical reactions are involved. Details can be found in Appendix 1 of the computer program manual.

2.2 Diffusion through the blade surface boundary layers

At the outer edge of the boundary layer, the pressure and temperature of the flow are assumed known and the concentrations of the species Na_2SO_4, NaCl, NaOH, NaO_2, K_2SO_4, KCl, KOH and KO_2 can be obtained as described in Section 2.1 using either the full equilibrium or frozen sulphate approximation. The mole fractions of all sodium and potassium species are extremely low and their presence does not affect the calculation of the carrier gas properties. The problem is to compute the rate at which the sodium and potassium species diffuse through the boundary layer and deposit in liquid or solid form on the metal surface of the turbine blade.

Because the Na and K species concentrations are very low, it is assumed that chemical reactions within the boundary layer do not occur and that the various salts diffuse through the boundary layer without chemical rearrangement. This is probably a very good assumption. It does not imply, of course, that the mole fractions of the species remain constant through the boundary layer because, if this were the case, there would be no concentration gradients providing the ‘driving force’ for diffusion and hence no mass transport of any species to the blade surface. Concentration gradients are established because the liquid or solid deposit on the blade surface is in steady-state contact with the gaseous species at the gas-deposit interface. This means that the sodium and potassium species in the gas phase at this interface are in chemical equilibrium at the blade surface temperature. The difference in composition between the gas in contact with the surface and the freestream gas at the outer edge of the boundary layer then provides the ‘driving force’ for diffusion.

The boundary layer itself is assumed to be two-dimensional and can be either laminar

or turbulent. The computer program VAPOURDEP has been written on the assumption that a suitable solution for the velocity and temperature distributions throughout the boundary layer covering the turbine blade surface is available from a separate calculation. The present version of VAPOURDEP interfaces with a well-known public domain boundary layer code originally developed at Stanford University and known as STANCOOL. STANCOOL allows the calculation of boundary layer growth in the presence of gas injection for film cooling and is therefore very suitable for coal-fired gas turbine calculations. A special version denoted STANDEP is supplied which prints to a file which can be read directly by VAPOURDEP.

The equations describing diffusion through the boundary layer are presented in Appendix 2 of the VAPOURDEP manual. Also included in the same appendix is a description of how the laminar diffusion coefficients for each species are calculated. Turbulent diffusion coefficients are obtained from the known eddy viscosity distribution and the common assumption that the turbulent Schmidt number is unity.

The species conservation equations are solved using a numerical, finite-volume approach. Firstly, it is necessary to establish a computational grid covering the flow domain. In common with all turbulent boundary layer problems it is important to solve the equations on a grid which becomes finer in the region close to the blade surface (where the concentration gradients are greatest) and the generation of such a non-uniform grid is described in Appendix 3 of the manual. Appendix 4 then describes how the numerical solution is achieved by marching along the blade surface, station-by-station, solving the equations across the boundary layer at each station using an implicit matrix method. In order to start this procedure, initial estimates of the concentration profiles are required and Appendix 5 describes how these are generated. The final part of the diffusion calculation is to deduce the mass transfer coefficient for each species from the numerical solution and the method by which this is done is detailed in Appendix 6.

2.3 Equilibrium at the gas-deposit interface

Knowing the mole fractions of a given species in the gas phase, both at the blade surface and in the freestream, together with the relevant mass transfer coefficient, allows the rate of transport to the surface of that species to be determined. The calculation of the freestream mole fractions has been described in Section 2.1 and the mass transfer coefficients in Section 2.2. Here, the condition at the blade surface is addressed.

At the blade surface, the program implements a special thermo-chemical boundary condition which assumes the existence of a liquid or solid deposit on the metal. At present, the user must specify whether the deposit is liquid or solid. The main assumption of the theory is that the Na and K species in the gas phase in contact with the deposit are in

equilibrium with each other and also with the components of the deposit. It is further assumed that the deposit is composed of Na_2SO_4 and K_2SO_4 only. Even when chlorine is present, calculations have indicated this to be a good approximation in most practical situations.

Calculation of the equilibrium composition in the gas phase is straightforward once the mole fractions of Na_2SO_4 and K_2SO_4 in the deposit are known. The method involves the application of Raoult's law with modifications for non-ideal behaviour and ionic dissociation in the liquid or solid deposit and is described in Appendix 7 of the VAPOURDEP manual. The rate of deposition of Na_2SO_4 and K_2SO_4 can then be obtained by use of the mass transfer coefficients and the known freestream gas composition.

The dewpoint temperature is defined as the surface temperature above which a stable liquid or solid deposit cannot form (*i.e.*, any deposit present will evaporate). At the dewpoint temperature, the fluxes to the surface of Na and K are independently zero. By iterating simultaneously on the surface temperature and the mole fraction of Na_2SO_4 in the deposit (while assuming the local free-stream mole fractions and the mass transfer coefficients remain unaltered), it is possible to calculate the dewpoint temperature at each station along the blade surface. Comparison with the actual blade temperature then shows whether or not a deposit will form and hence whether or not corrosion of the blade metal is likely.

3 THE COMPUTER PROGRAM 'VAPOURDEP'

The computer program is written in FORTRAN 95 and a user manual is appended at the end of this part of the Final Report. This manual formed the Milestone 1 Report of the project. It gives details of how to run the code, the input data requirements and a description of the output. The appendices describe the governing equations and method of solution as discussed in Section 2 above. The program is about 2500 lines long and is extensively commented. It is straightforward to follow in parallel with the description in the manual.

4 TESTING AND VALIDATION OF THE PROGRAM

One of the aims of the Project was that the industrial partners should apply the codes developed at Cambridge to relevant problems, thereby gaining experience in using the codes as well as generating useful information on deposition. This section describes the application by Powergen of the new vapour deposition code to the same example utility turbine as used in the previous Topping Cycle work. The results of the new code were compared to the original results for high chlorine coal. Then the new code was used to look at the effects of different chlorine and sulphur concentrations and the effects of different levels of alkali.

4.1 Utility turbine test case

The Topping Cycle utility turbine was used because the flow conditions in the turbine were already known in detail, thus saving considerable work in not having to perform flow calculations. A summary of the flow conditions through the turbine is given in Table 4.1.

Position	Total Pressure (bar)	Total Temperature (°C)
Inlet	13.62	1380
Stator 1 LE	13.62	1380
Stator 1 TE	12.93	1260
Rotor 1 LE (relative)	7.92	1109
Rotor 1 TE (relative)	7.69	1073
Stator 2 LE	5.76	994
Stator 2 TE	5.57	953
Rotor 2 LE (relative)	3.78	853
Rotor 2 TE (relative)	3.68	841
Stator 3 LE	2.58	761
Stator 3 TE	2.52	745
Rotor 3 LE (relative)	1.73	662
Rotor 3 TE (relative)	1.70	664

Table 4.1: Conditions in the example utility turbine.

The base case gas and alkali conditions for the present work are taken from the 'worst case' scenario of the original utility turbine calculations, Reference [1]. This was derived specifically from certain assumptions about the air-blown gasification system, but here the case is just used as a typical starting point to examine the effects of varying gas composition on alkali deposition. The gas composition entering the turbine (*i.e.*, at the outlet to the combustor) is given in Table 4.2.

Component	molar (volume) fraction
N_2	0.71
H_2O	0.12
O_2	0.08
CO_2	0.09
SO_x	140×10^{-6}
HCl	110×10^{-6}
Na	24×10^{-9}
K	42×10^{-9}

Table 4.2: Base case gas composition.

The values in the table are for a typical UK coal. The level of HCl of 110 ppmv (parts per million by volume) would be higher than for many international coals, so this base case can be considered as an example with a high chlorine content.

4.2 Comparison with original code for high chlorine coal

The original model for vapour deposition assumed that the alkali in vapour form could only include the chloride, hydroxide and sulphate salts. With the high level of chlorine, equilibrium at the combustor outlet temperature then leads to the chloride being the dominant gas-phase salt species, followed by the hydroxide, with the sulphate concentration being much lower. It was assumed in the original work that, having come to equilibrium at the combustor outlet temperature, the relative proportions of the different salts remained frozen through the rest of the turbine, concentrations only being altered by the added cooling air. The time to traverse the turbine is quite short (of the order of 1 ms) and the alkali concentrations are very low, so this assumption seems quite reasonable and is retained for the present calculations. However, the new model allows four species of salts to be considered by including the superoxides (NaO_2 and KO_2). The difference that this produces in the vapour salt concentrations for the base case is illustrated in Table 4.3.

For this high chlorine case, the chloride salts dominate with both the present and original models. The relative levels between the chlorides, hydroxides and sulphates is similar for both models, but the new model shows that the superoxide salts make a significant contribution, being intermediate between the chlorides and hydroxides in concentration.

Salt	Original code Mole fraction	Present code Mole fraction
NaCl	2.1×10^{-8}	1.6×10^{-8}
NaOH	2.4×10^{-9}	1.8×10^{-9}
Na_2SO_4	6.9×10^{-16}	9.6×10^{-16}
NaO_2	-	5.3×10^{-9}
KCl	3.8×10^{-8}	3.1×10^{-8}
KOH	4.0×10^{-9}	3.2×10^{-9}
K_2SO_4	1.6×10^{-15}	2.6×10^{-15}
KO_2	-	7.3×10^{-9}

Table 4.3: Alkali salt concentrations at turbine inlet conditions (high chlorine content).

For estimating deposition, a solid or liquid deposit is assumed on the blade surface. Then the sodium and potassium species in the gas phase directly in contact with the deposit are assumed to be in thermodynamic equilibrium with each other and with the components of the deposit, all taken to be at the blade surface temperature. The original code allowed the possibility of sulphate or chloride salts in the deposit, but the results from it consistently showed that the deposit was almost entirely composed of the sulphates. An assumption of only sulphates in the deposit has been built into the present code to make the application of the fairly complicated thermo-chemical boundary conditions easier.

The code then calculates the composition of the deposit and the mole fractions of the sodium and potassium species in the gas at the interface with the deposit. The difference in mole fractions across the boundary layer together with the mass transfer coefficients (calculated from the input flow data) gives the fluxes of the various species to or from the surface. If the net flux is away from the surface, this indicates that any deposit is evaporating (and hence there will be no deposit). If the net flux is towards the surface, then deposition is occurring. At one particular surface temperature there will be zero net flux and this is taken to be the dewpoint temperature.

The alkali salt deposition rates on all the blade leading edge regions through the turbine have been calculated for varying blade temperatures using both codes. The mass transfer coefficients have been obtained from established empirical correlations, so the flow element is removed from the two codes and this test just compares the two different thermo-chemical models used. Figure 4.1 shows the results of the calculations with the two codes in terms of the net alkali salt flux rate plotted against blade surface temperature.

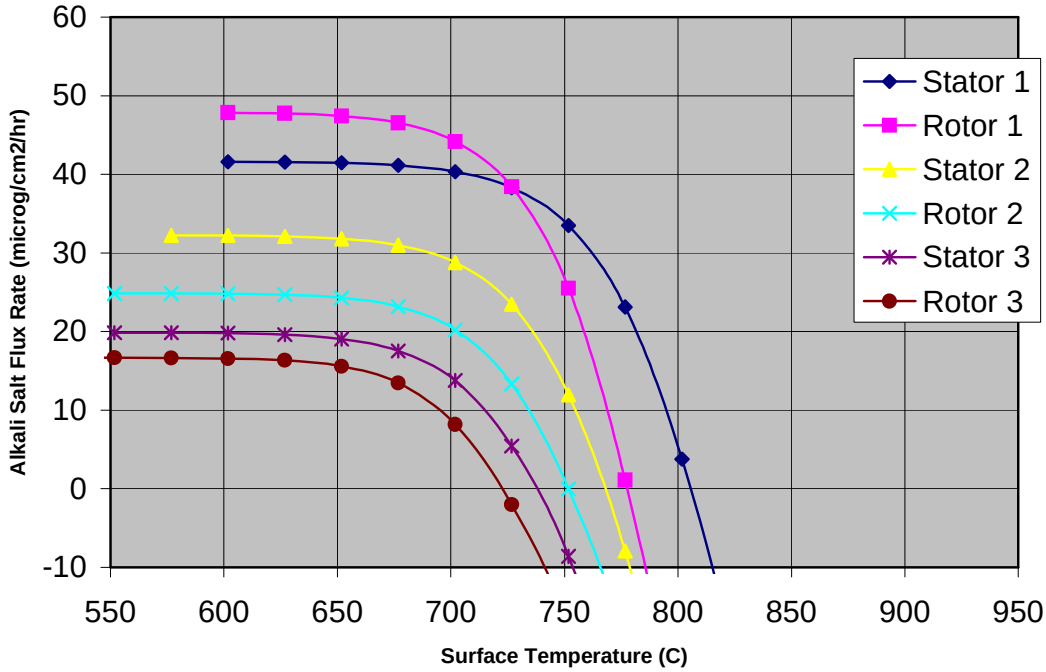

(a) Original calculation.

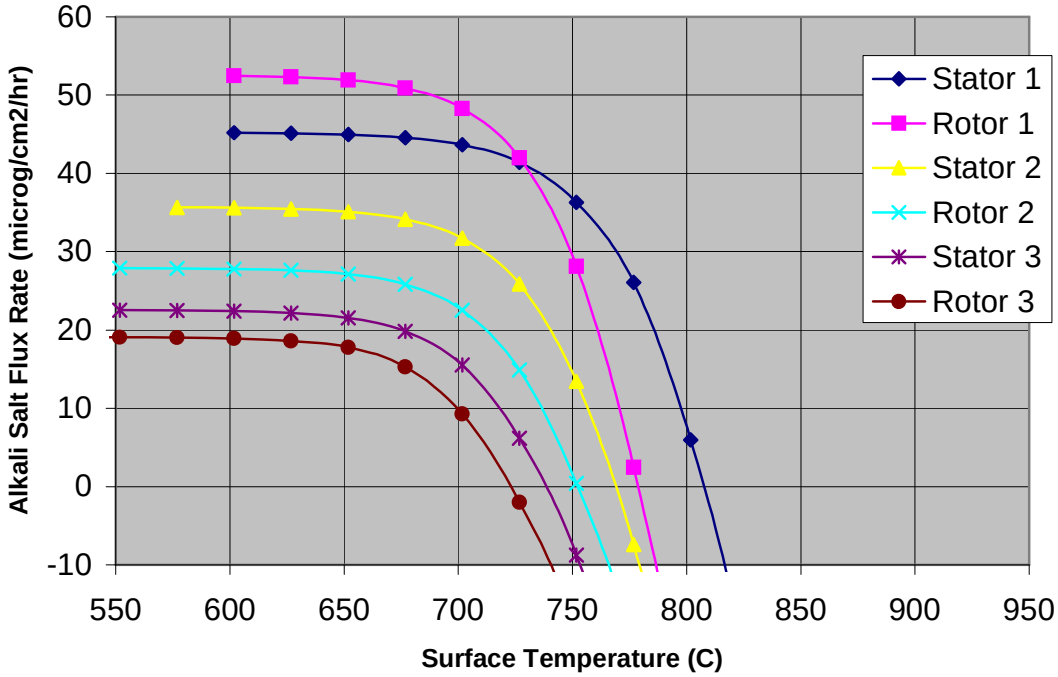

(b) New calculation.

Figure 4.1: Net sodium/potassium salt deposition rates on utility GT leading edge regions.

All the curves show the same general variation with surface temperature. At high temperatures, the flux rates are negative indicating evaporation (so that, in practice, no deposit would occur). As the temperature decreases the flux rates increase, passing through zero at the dewpoint temperature, and then tend towards almost constant 'plateau' values at low temperatures. This behaviour can be explained because, at the lower temperatures, the salt concentrations in the gas directly in contact with the deposit are so much lower than those at the outer edge of the boundary layer that the concentration difference responsible for the mass transfer is essentially determined solely by the free stream concentrations. This means that the flux rates become independent of the surface temperature and also do not depend to any great extent on the deposit chemistry. The plateau levels are lower for later blade rows in the turbine because the molar densities of the salts decrease in passing through the machine, in line with the reduction in overall gas density. This reduces the concentration differences driving the mass transfer and hence the plateau deposition levels are lower in later blade rows.

As shown in Fig. 4.1, the only exception to this tendency is in the first stage, where the rotor blade has a higher plateau level than the stator blade. This is because the relative velocity at inlet to the first rotor row is much higher than the velocity at inlet to the first stator row. The stagnation mass transfer coefficient is consequently much higher for the rotor and more than compensates for the reduction in pressure. The dewpoint temperatures (corresponding to zero net sodium and potassium fluxes) also reduce through the machine because of the reduction in pressure. This does not, however, reduce the risk of deposition in the later stages, since blade temperatures fall more rapidly than the dewpoint temperatures. A secondary effect tending to reduce the deposition rates through the machine is due to the dilution produced by the addition of cooling air from blades and rotor discs being added to the mainstream flow.

The results from the two codes agree fairly closely, as one would hope for this high chlorine case. Indeed, the dewpoint temperatures predicted by the two codes for the different blade rows are almost identical. The main difference between the two calculations is that the plateau levels at the lower temperatures are slightly higher with the new code. This is because of the different salt species in the mainstream gas flow. The superoxide, which the new code allows to be present, has a higher diffusion coefficient than the hydroxide, and this leads to the overall mass transfer rates being slightly greater.

Some detailed flow results were available for the first stage stator blade of the utility turbine. Figure 4.2 gives plots of the velocity around the blade (external to the boundary layer) and of the surface temperature. The surface temperature varies widely because the blade is film cooled at several different locations. The temperature immediately downstream of each row of film cooling holes is low but then gradually creeps back up until the next row of holes is reached.

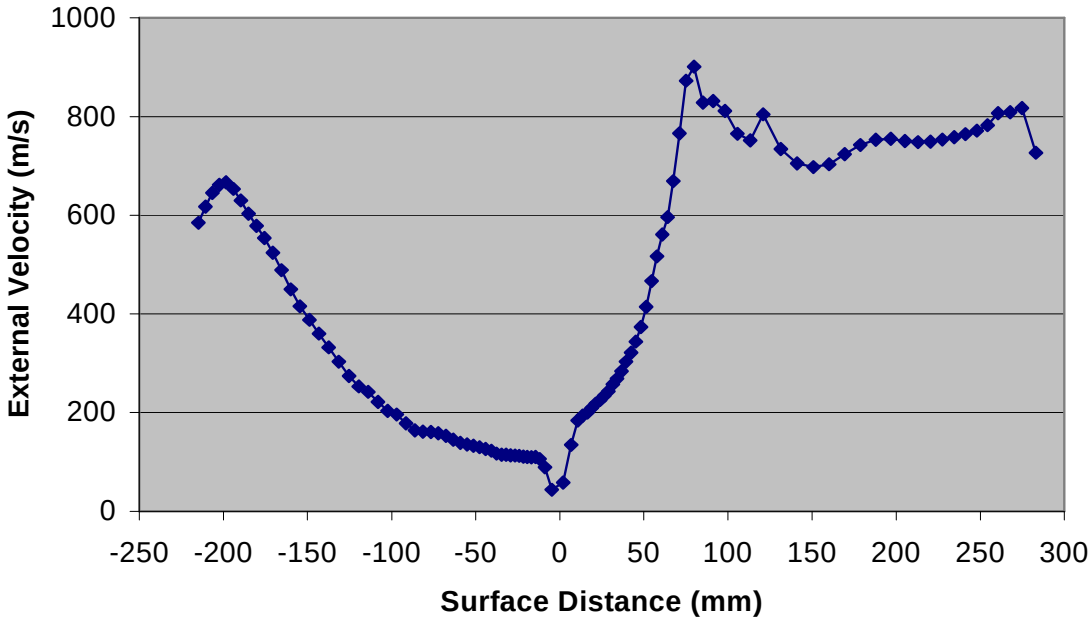

(a) Velocity distribution.

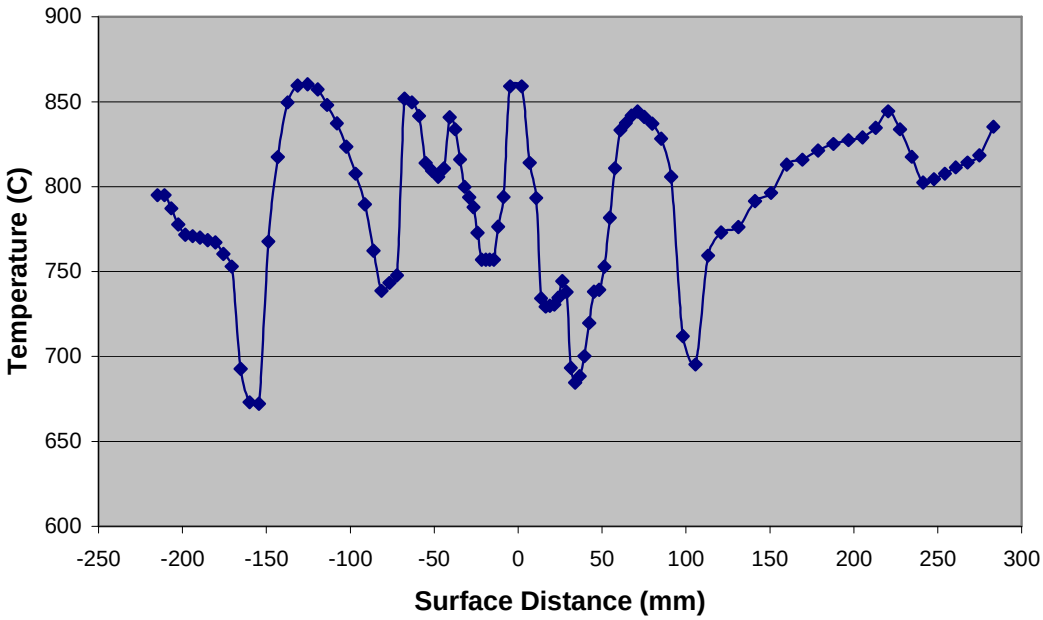

(b) Surface temperature distribution.

Figure 4.2: Utility gas turbine, first stage stator conditions.

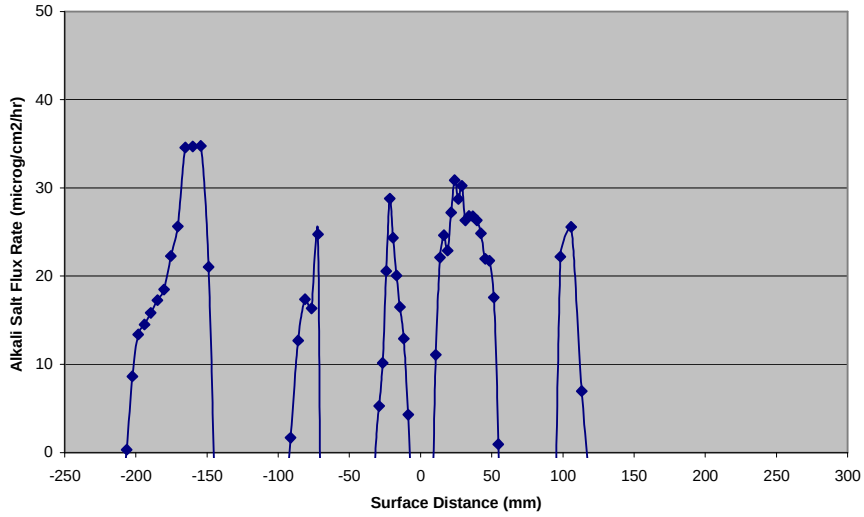

(a) Original calculation.

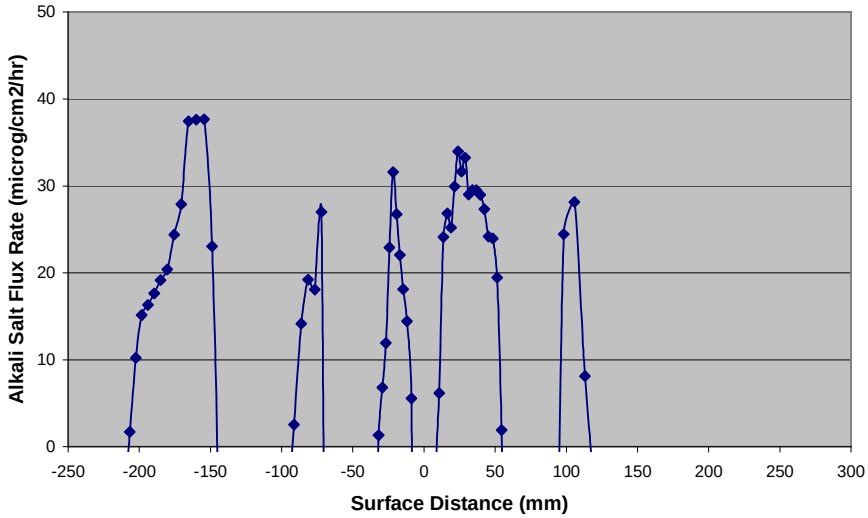

(b) New calculation.

Figure 4.3: Alkali deposition rates along surface of utility first stage stator blade.

Calculations of alkali deposition rates have been made for the stator blade with the base case gas composition using both the old and new codes. Figure 4.3 shows that the results from the two calculations are very similar. The new code has just slightly higher deposition rates, for the reasons given above. It should be noted that deposition only occurs in those regions where the surface temperature is below the local dewpoint temperature.

4.3 Effect Of varying the chlorine levels

Having established that the new code produces similar results to the previous code for a high chlorine case, it was decided to investigate the effect of reducing chlorine concentrations. The original code would not be accurate for low chlorine concentrations because of the assumptions built into it, but the new code should be able to handle such cases. For this test, the HCl concentration was reduced by a factor of 10, from the base case level of 110 ppmv to 11 ppmv. The predicted vapour salt concentrations entering the turbine with this lower chlorine level are given in Table 4.4. In this case, the superoxide is the dominant salt species, with the hydroxide and chloride being at a lower level.

Salt	Mole fraction
NaCl	4.4×10^{-9}
NaOH	4.9×10^{-9}
Na_2SO_4	6.9×10^{-15}
NaO_2	1.4×10^{-8}
KCl	9.5×10^{-9}
KOH	9.8×10^{-9}
K_2SO_4	2.4×10^{-14}
KO_2	2.2×10^{-8}

Table 4.4: Alkali salt concentrations at turbine inlet conditions (low chlorine content).

The results from the new code for the leading edge deposition rates with the high chlorine base case are reproduced in Fig. 4.4(a) for comparison with the results for the low chlorine case in Fig. 4.4(b). The low temperature plateau levels are almost the same for the two chlorine levels, the different composition of the salt vapours in the free stream having very little effect. There is, however, a considerable change in the dewpoint temperatures, with the low chlorine case having dewpoint temperatures around 50°C higher. This could be very significant in bringing more blade rows, or parts of a blade surface, below the dewpoint temperature with the result that deposition occurs there.

This is illustrated by Fig. 4.5 which gives deposition rates on the utility stator for the two chlorine levels, (both calculated with the new code). Although, the deposition rates are of similar magnitude for the two cases, there is deposition occurring on far more of the blade surface in the low chlorine case, because more of the surface is below the dewpoint temperature.

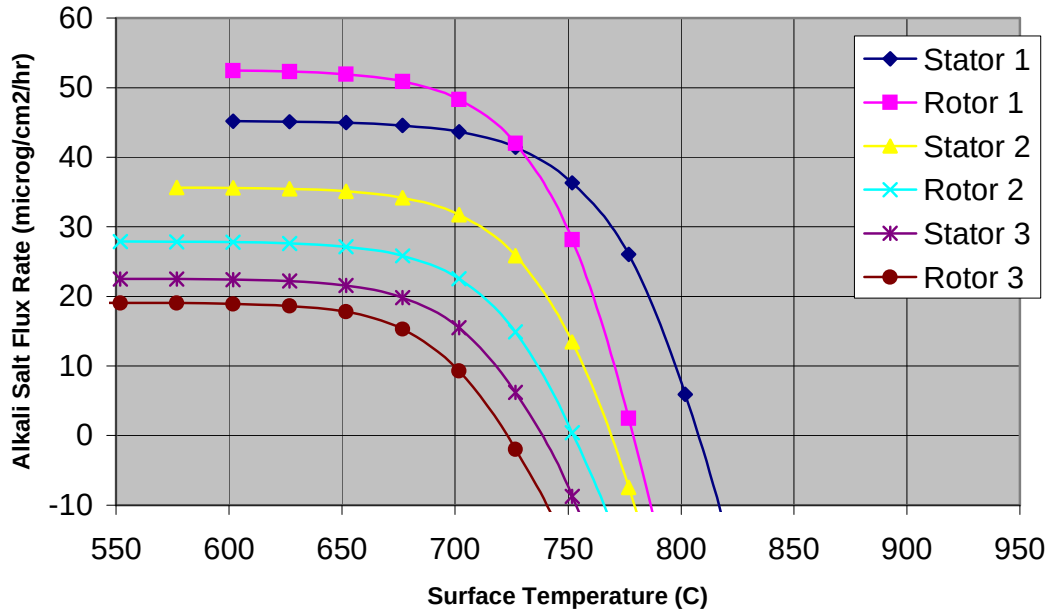

(a) High chlorine content.

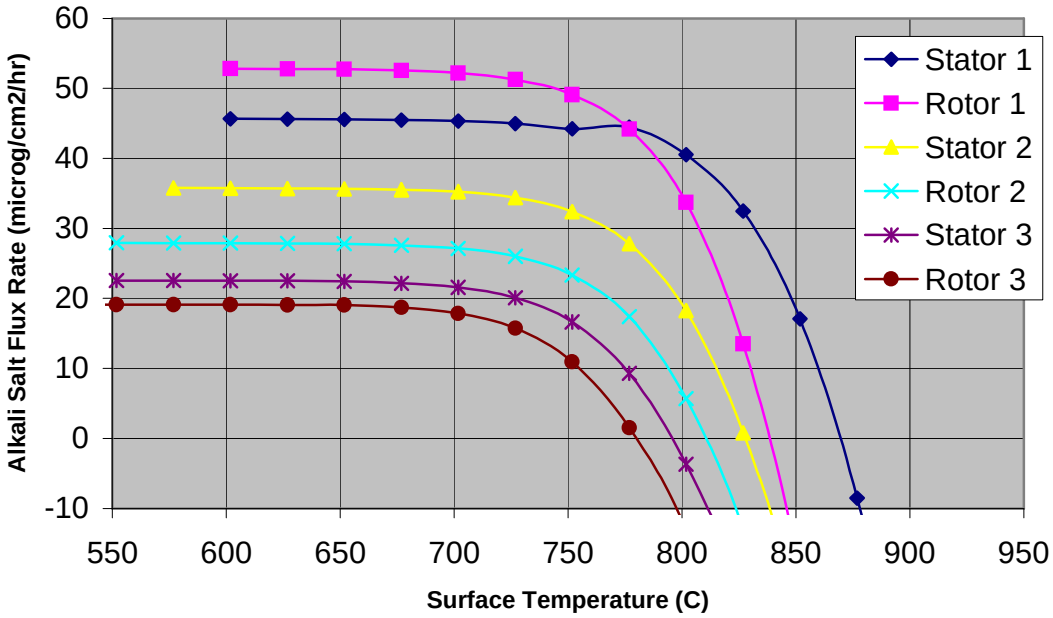

(b) Low chlorine content.

Figure 4.4: GT leading edge deposition rates for different chlorine levels.

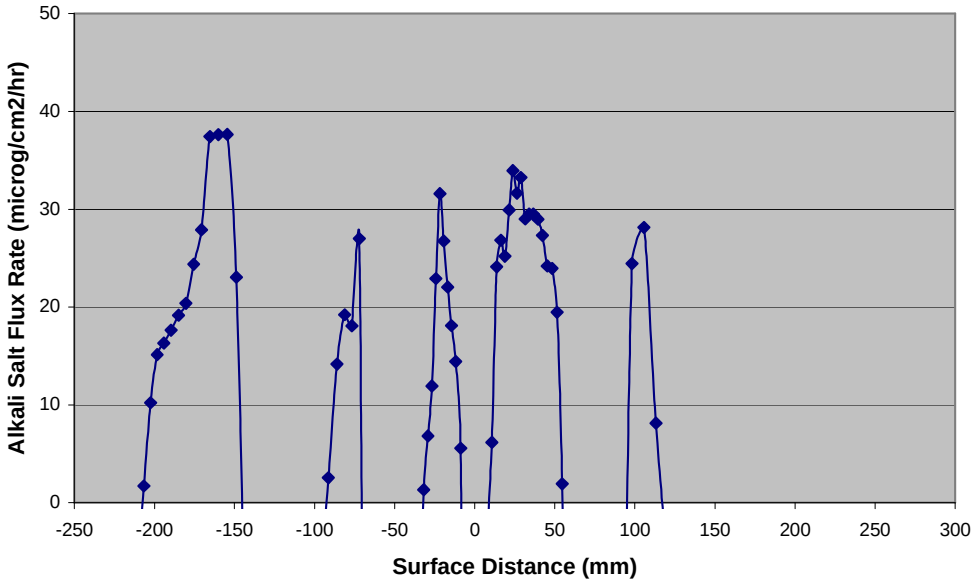

(a) High chlorine content.

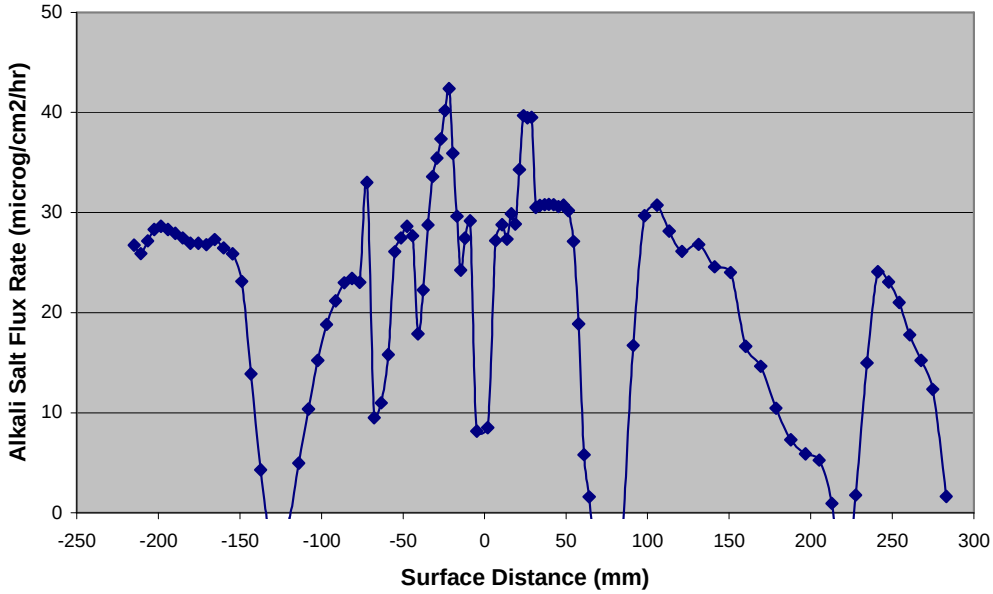

(a) Low chlorine content.

Figure 4.5: Deposition rates for utility stator blade for different chlorine levels.

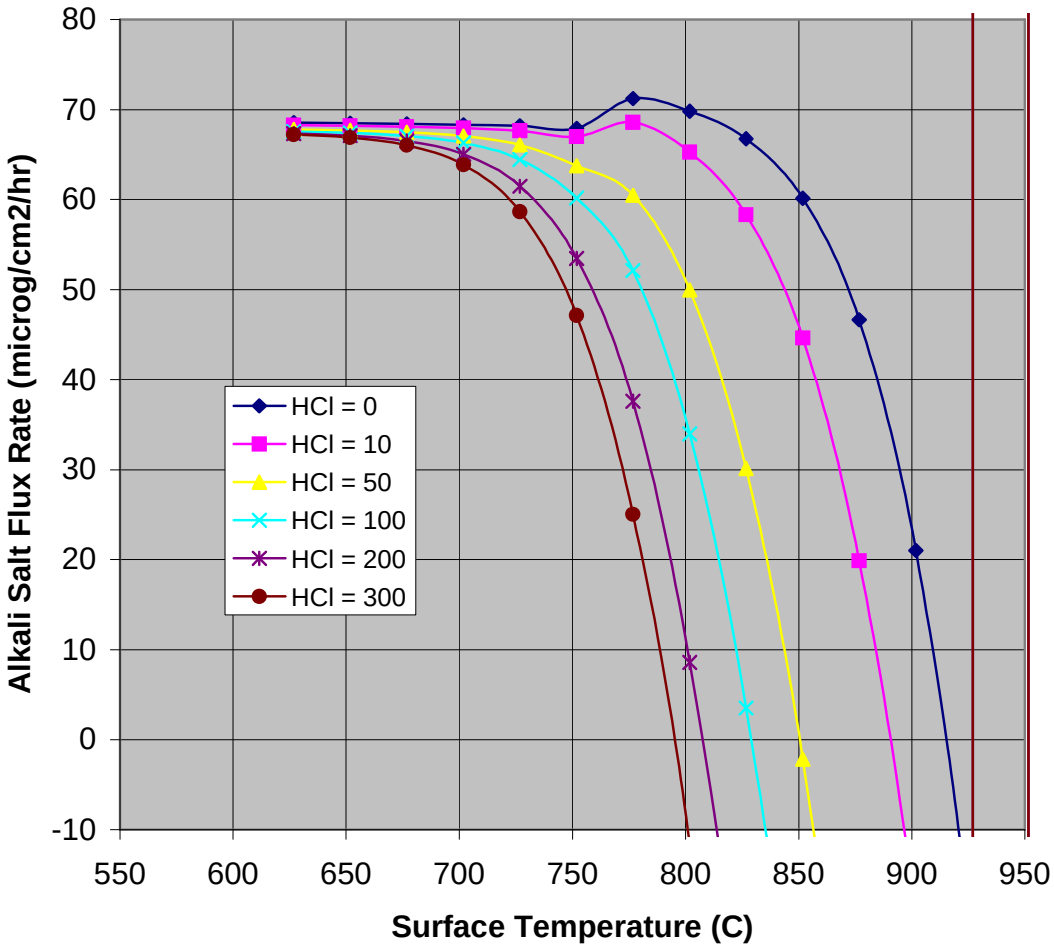

Figure 4.6: First stage stator leading edge deposition rates for varying chlorine levels.

In Fig. 4.6, the deposition rates on the first stage stator leading edge are plotted against surface temperature for different chlorine levels from 0 to 300 ppmv. This clearly shows the increase in dewpoint temperature with decreasing chlorine level. The low temperature plateau levels vary only slightly, tending to be marginally greater for lower chlorine levels.

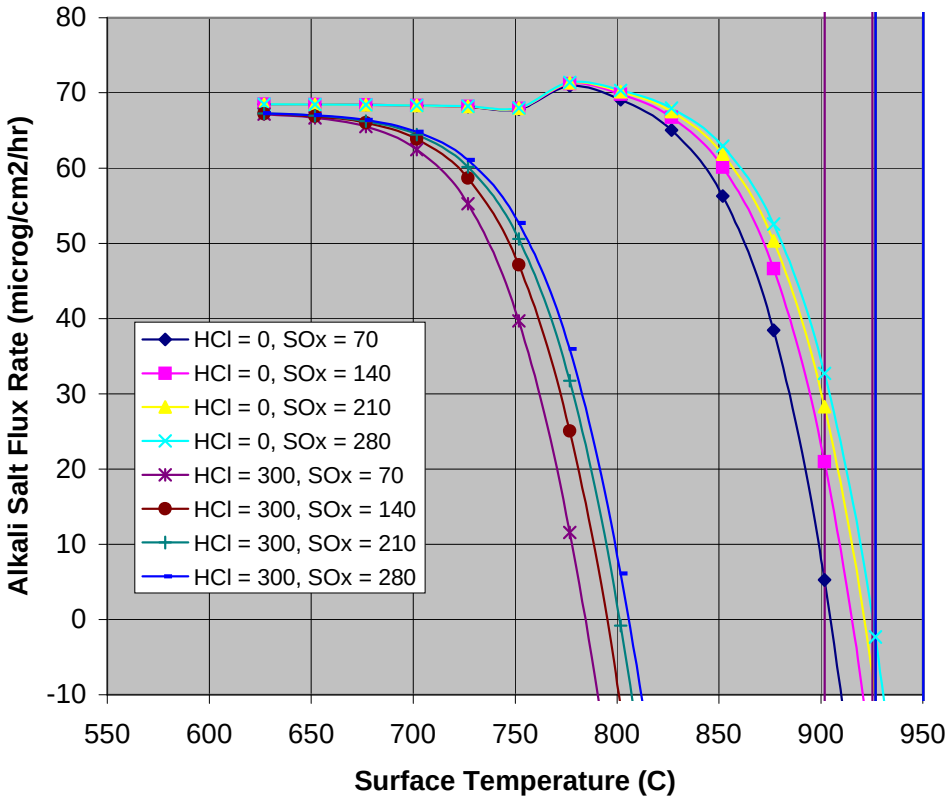

Figure 4.7: First stage stator leading edge deposition rates for varying sulphur levels.

4.4 Effect of varying the sulphur levels

The new code has also been applied to study the effect of varying sulphur levels. Figure 4.7 gives the deposition on the leading edge of the first stage stator for different SO_X levels from 70 to 280 ppmv. This has been done for the two extreme chlorine levels of zero and 300 ppmv. The effect of changing the sulphur level is similar at both chlorine levels, with the dewpoint increasing with increasing sulphur (the opposite of the effect with chlorine) and the low temperature plateau levels being virtually unchanged.

4.5 Effect of varying the alkali levels

Figure 4.8 shows the effect of varying the alkali levels for the two extreme chlorine cases. Again, the behaviour at the two chlorine levels is very similar. With the alkali split equally between sodium and potassium, doubling the alkali level from 50 ppbv (parts per billion by volume) of each to 100 ppbv increases the low temperature plateau level in direct proportion (as might be expected), and also increases the dewpoint by about 20°C. Two other cases with different relative proportions of alkali were also computed; with sodium four times the potassium level and vice versa. The case with the higher proportion of sodium has a lower plateau level and a higher dewpoint temperature than the high potassium case.

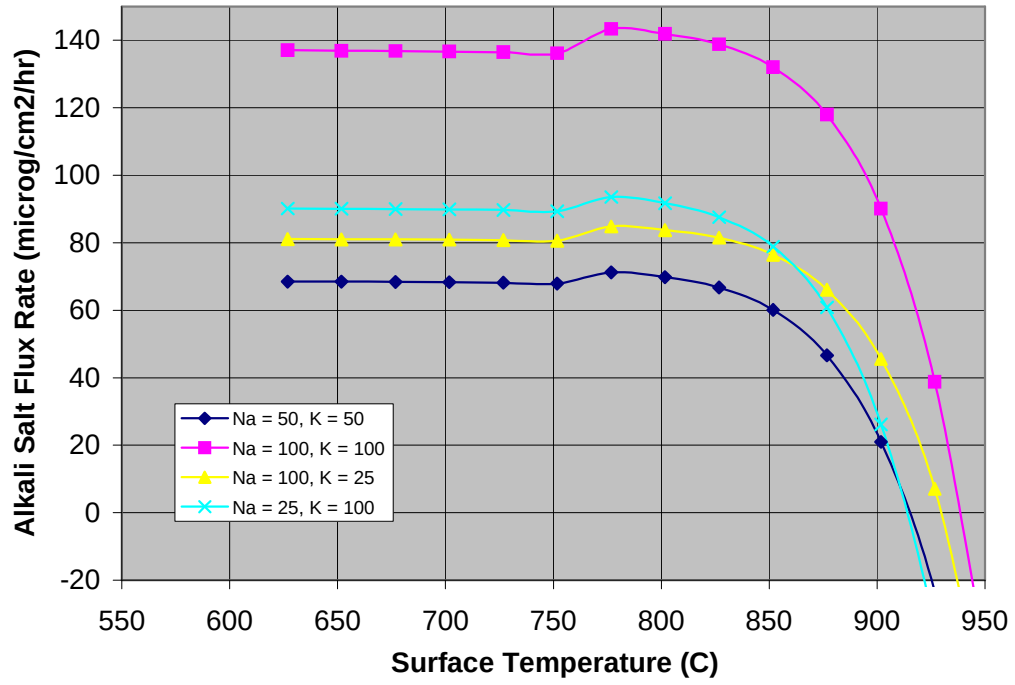

(a) zero HCl concentration.

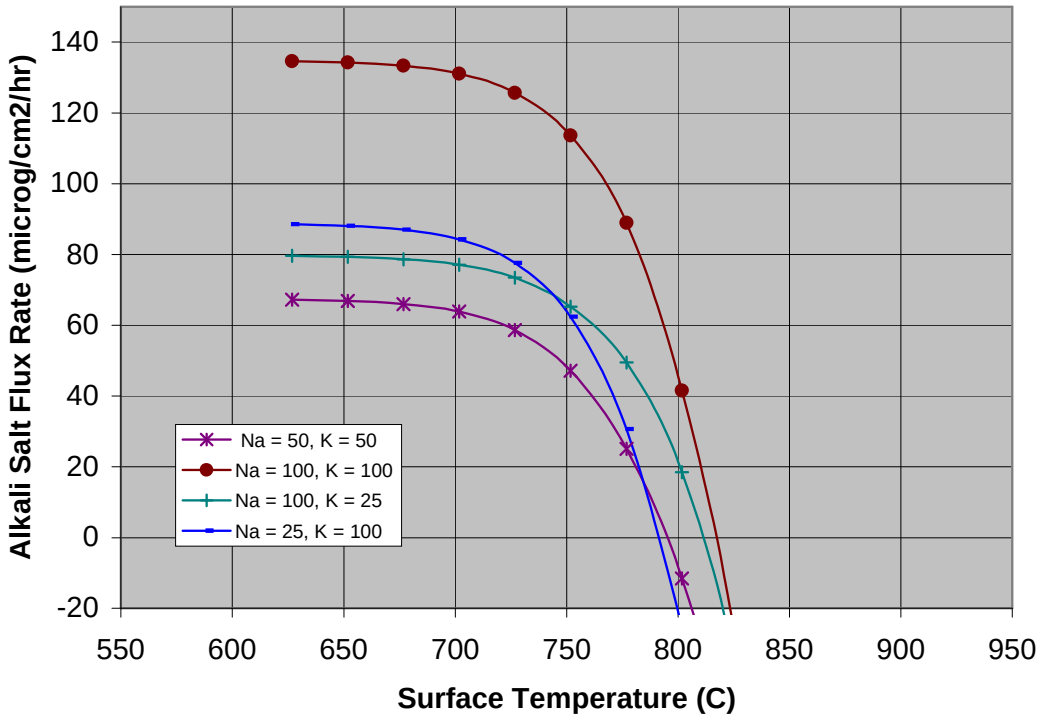

(b) HCl concentration of 300 ppmv.

Figure 4.8: First stage stator leading edge deposition rates for varying alkali levels.

4.6 Conclusions from the studies

1) For high chlorine content, the new code predicts very similar results to the original one, giving just slightly higher deposition rates but almost identical dewpoint temperatures.

2) As chlorine levels are reduced, the dewpoint temperatures increase significantly, but the almost constant plateau deposition rates at temperatures well below the dewpoint hardly change, just increasing very slightly.

3) Increasing the sulphur level produces an increase in dewpoint temperature (opposite from the effect of chlorine), but the plateau levels are again hardly affected.

4) Increasing the alkali levels increases the dewpoint temperatures and increases the plateau deposition rates proportionally. If there is a higher proportion of sodium than potassium then the plateau deposition rate is lower and the dewpoint temperature higher compared with a case involving a higher proportion of potassium.

REFERENCE

[1] 'Review of modelling for the GTCP and model predictions', Grimethorpe Topping Cycle Project Report GTCP/TR16, 1994.

VAPOURDEP

A computer program for calculating the rates of deposition of alkali metal salt vapours from 2-D boundary layers on gas turbine blades

USER MANUAL

J.B.YOUNG

Hopkinson Laboratory
Cambridge University Engineering Department

VERSION 1.1

JULY 2004

INTRODUCTION

VAPOURDEP is a computer program written in FORTRAN 95 for calculating the rates of diffusion of sodium and potassium compounds, present in trace amounts in vapour form, through two-dimensional boundary layers on gas turbine blades. The code is based on a theoretical model developed by Dr. R. Tabberer and Dr. J.E. Fackrell of the PowerGen, Power Technology Centre, Ratcliffe-on-Soar.

VAPOURDEP itself only solves the conservation equations for the sodium and potassium species subject to certain boundary conditions. The velocity and temperature fields within the boundary layer are not computed by VAPOURDEP and must be specified externally. This is achieved by interfacing with the well-known boundary layer code STANCOOL developed at Stanford University. A special version of STANCOOL, denoted STANDEP, is supplied which prints output to a file which can be read directly by VAPOURDEP.

The input data file to STANDEP is unchanged from the original program. However, it should be appreciated that VAPOURDEP will only deal with plane two-dimensional, laminar and turbulent, external boundary layers. When specifying the input data for STANDEP, only those options should be employed which are compatible with the possible modes of operation of VAPOURDEP.

When running STANDEP, the following I/O streams must be connected :

UNIT 2 Output results file to be read directly by VAPOURDEP.
UNIT 3 Table of carrier gas property values for input to STANDEP.
UNIT 4 Output results file from STANDEP for printing.
UNIT 10 Main input data file for STANDEP.

When running VAPOURDEP, the following I/O streams must be connected :

UNIT 1 Input data file for VAPOURDEP.
UNIT 2 Results file output by STANDEP on UNIT 2.
UNIT 8 Output results file from VAPOURDEP for printing.

PROGRAM DETAILS

Carrier gas components

The mole fractions of the carrier gas components are specified by the user as input data and it is assumed that the composition remains constant throughout the flowfield. The program will accept four components, numbered as follows :

1. Nitrogen (N_2)
2. Carbon dioxide (CO_2)
3. Water vapour (H_2O)
4. Oxygen (O_2)

The mole fractions of these components should sum to unity and their mean molar mass should be identical to the mean molar mass used for the STANDEP calculation. It is up to the user to ensure that this is so as no internal check is made. N_2, H_2O and O_2 must be present but CO_2 may be absent.

Sulphur and chlorine

The mole fractions of atomic sulphur and chlorine present (typically of order 10^{-5}) are specified by the user. The program then assumes that all sulphur is present as SO_2 and all chlorine as HCl, numbered as follows :

5. Sulphur dioxide (SO_2)
6. Hydrogen chloride (HCl)

Sulphur must be present but chlorine may be absent.

Sodium and potassium compounds

The mole fractions of atomic sodium and potassium (typically of order 10^{-8}) are specified by the user. The program then calculates the gas-phase equilibrium composition assuming the following species may be present :

1. Sodium sulphate (Na_2SO_4)
2. Sodium chloride (NaCl)
3. Sodium hydroxide (NaOH)
4. Sodium superoxide (NaO_2)
5. Potassium sulphate (K_2SO_4)
6. Potassium chloride (KCl)
7. Potassium hydroxide (KOH)
8. Potassium superoxide (KO_2)

Details of the gas-phase equilibrium calculations are given in Appendix 1.

Species conservation equations and method of solution

The derivation of the conservation equations for the sodium and potassium species in 2D laminar or turbulent boundary layers can be found in Appendix 2. Only concentration diffusion is modelled and thermal diffusion is not included. The method of solution employed is a second-order accurate finite volume technique described in Appendix 3. The grid generation is described in Appendix 4.

Initial concentration profiles

The initial concentration profile can either correspond to the flow over a flat plate with zero pressure gradient (set IPROFIL = 0 in the input data) or to the flow near a stagnation point (set IPROFIL = 1). Whether the initial profile represents a laminar or turbulent boundary layer depends on information automatically passed from the STANDEP solution. If a laminar profile is required, a similarity solution is generated using the Falkner-Skan transformation. If a turbulent profile is required, a special procedure is employed to generate a profile which closely approximates the 'concentration law of the wall'. Details can be found in Appendix 5.

Film cooling gas injection

Gas injection due to film cooling is computed by VAPOURDEP without user intervention as all film cooling information is automatically passed to VAPOURDEP from the STANDEP solution. At each film cooling location, the diffusion calculations are temporarily suspended, only to be restarted downstream of the coolant injection holes with freshly generated initial concentration profiles. The method used to calculate these profiles is the same as that used to generate the initial concentration profile for a turbulent boundary layer on a flat plate and is described in Appendix 5. This approach is not ideal but it is difficult to conceive of a scheme which will establish more reliable restart conditions. It should be noted that the addition of coolant alters the gas composition and the values of the diffusion coefficients but this is not accounted for in the calculations.

Calculation of the mass transfer coefficients

The mass transfer coefficients of the sodium and potassium species are calculated both by a differential method (evaluation of the concentration gradient at the blade surface) and an integral method (rate of increase of the concentration thickness). A comparison of the two results gives some indication of the accuracy of the finite volume discretization. The definitions and methods of calculation of the mass transfer coefficients and Sherwood numbers are given in Appendix 6.

Surface boundary conditions

At the blade surface, a special thermo-chemical boundary condition is applied corresponding to the existence of a thin liquid or solid deposit. The program then calculates the composition of the deposit and the mole fractions of the sodium and potassium species in the gas at the gas-deposit interface. Knowing the difference in mole fractions across the boundary layer together with the mass transfer coefficients allows the calculation of the molar fluxes of the various species to or from the surface. If, at the particular surface temperature specified, it is found that the net sodium and potassium fluxes are directed away from the surface, this implies that any deposit present will be evaporating. If, on the other hand, the net fluxes are directed towards the surface then condensation will be occurring and the deposit will be increasing in thickness. For one particular value of the surface temperature it will be found that the net fluxes of sodium and potassium are both zero. This temperature is known as the dewpoint temperature. The interpretation is that, if the surface temperature is above the dewpoint temperature, no alkali salt deposit will form on the blade. Further details of the theory underlying the application of the thermo-chemical boundary condition can be found in Appendix 7.

Thermodynamic and transport properties

A list of the SUBROUTINES for calculating the thermodynamic and transport properties required by VAPOURDEP is given in Appendix 8.

Dimensioning of arrays

The dimensioning of arrays is controlled by the PARAMETER statements in MODULE PARAMETERS. The following parameters are specified :

kstz = Maximum number of grid points across BL in STANDEP calculation.
nstz = Maximum number of *x*-stations along blade in STANDEP calculation.
kpz = Maximum number of grid points across BL in VAPOURDEP calculation.
ngas = Number of gas components.
nsalt = Number of sodium and potassium species.
nreac = Number of gas-phase chemical reactions.

UNIT 1 INPUT DATA

(Free format)

```
INTEGER          :: iequm, deposit, iprofil, kpoint
INTEGER          :: nprint, mprint, nprofil, mprofil, maxprofil
REAL*8           :: XN2, XCO2, XH2O, XO2, XSULPH, XCHLOR, XSOD, XPOT
REAL*8           :: PCOMB, TCOMB, SCHTRB, TURBN, YWPLUS, BLINC
CHARACTER*70 :: Ctitle*70
```

```
READ (1,*)    Ctitle
READ (1,*)    PCOMB, TCOMB
READ (1,*)    XN2, XCO2, XH2O, XO2
READ (1,*)    XSULPH, XCHLOR, XSOD, XPOT
READ (1,*)    iequm, deposit
READ (1,*)    SCHTRB, TURBN
READ (1,*)    iprofil, kpoint, YWPLUS, BLINC
READ (1,*)    nprint, mprint
READ (1,*)    nprofil, nprofil, maxprofil
```

Ctitle	=	Title of 70 characters or less (must be enclosed in quotation marks).
PCOMB	=	Combustor outlet pressure (Nm^{-2}).
TCOMB	=	Combustor outlet temperature (K).
XN2	=	Mole fraction of N_2
XCO2	=	Mole fraction of CO_2
XH2O	=	Mole fraction of H_2O
XO2	=	Mole fraction of O_2
XSULPH	=	Mole fraction of atomic sulphur (combustor outlet).
XCHLOR	=	Mole fraction of atomic chlorine (combustor outlet).
XSOD	=	Mole fraction of atomic sodium (combustor outlet).
XPOT	=	Mole fraction of atomic potassium (combustor outlet).
iequm	=	1 – Full chemical equilibrium in the free-stream throughout turbine.
	=	2 – Frozen sulphates in the free-stream.
deposit	=	1 – Program assumes deposit is liquid.
	=	2 – Program assumes deposit is solid.
SCHTRB	=	Turbulent Schmidt number, assumed constant everywhere (usually 1.0).

TURBN = Value of parameter *n* used to generate initial concentration profiles in a turbulent BL after film cooling gas injection (see Appendix 5). Values of 0.7 – 0.8 (depending on the Reynolds number) give accurate initial profiles for flat plate boundary layers with zero pressure gradients.

iprofil = 0 – Initial concentration profile is a self-similar solution for a flat plate with zero pressure gradient ($du_\infty/dx = 0$).

1 – Initial concentration profile is a self-similar solution for a stagnation point flow ($u_\infty = Cx$).

1) The choice of laminar or turbulent initial profiles follows automatically from information passed via the STANDEP output.
2) Laminar profiles correspond to Falkner-Skan similarity solutions.
3) Turbulent profiles correspond reasonably well to the 'concentration law of the wall' in the inner part of the BL but should be treated cautiously.
4) The input data value of iprofil refers only to the first *x*-station. After film cooling, iprofil = 0 is automatically selected.

kpoint = Number of computational points across boundary layer (typically 50).

YWPLUS = Value of $y_+ = yu_*/\nu$ at first computational point next to the surface.

1) YWPLUS is used to establish the grid spacing normal to the blade surface for both laminar and turbulent boundary layers.
2) Typically, YWPLUS = 0.1 – 0.2.
3) Do not take the Schmidt numbers into consideration when choosing YWPLUS as this is automatically handled by the program.

BLINC = If the grid does not extend far enough from the blade surface, the first action taken is to increase its extent by a factor BLINC. If this is insufficient, extra points are then added one by one. Typically, BLINC = 1.02 – 1.05.

The following variables control output to UNIT 8 :

nprint = n – Printing of main results starts at *x*-station n.
Note that first station is n = 0.

mprint = m – Main results are printed every m *x*-stations.
mprint = 1 gives output every step.

nprofil = n – Printing of concentration profiles starts at *x*-station n.

mprofil = m – Concentration profiles are printed every m *x*-stations.

maxprofil = Maximum number of profiles to be printed (used to avoid large files).

UNIT 2 INPUT DATA

(Fixed format, generated automatically by STANDEP)

```
-----------------------------------------------------------------------------------------------------
INTEGER                                  ::  k, n, nxend, imode, ifilm, kdum
INTEGER,        DIMENSION(nstz)          ::  intg, mfilm, kst
REAL*8,         DIMENSION(20)            ::  AUX1, AUX2, AUX3
REAL*8,         DIMENSION(20)            ::  AUX4, AUX5, AUX6
REAL*8,         DIMENSION(nstz)          ::  X, UE, PE, CF, DEL1, DEL2
REAL*8,         DIMENSION(kstz,nstz)     ::  YSTAN, ROSTAN, TSTAN
REAL*8,         DIMENSION(kstz,nstz)     ::  USTAN, MUSTAN, EVSTAN
-----------------------------------------------------------------------------------------------------
      DO  n = 1, nstz
         READ (2,200)  nxend,  imode,  mfilm(n),  intg(n),  kst(n)
200      FORMAT (1X, 5I5)
         READ (2,210)  X(n),  UE(n),  PE(n),  CF(n),
    &                  USTAR(n),  DEL1(n),  DEL2(n)
210      FORMAT (1X, 7E12.5)
         IF (mfilm(n) .GT. 0) THEN
            READ (2,220)  AUX1(ifilm),  AUX2(ifilm),  AUX3(ifilm)
   &                      AUX4(ifilm),  AUX5(ifilm),  AUX6(ifilm)
220         FORMAT (1X, 6E12.5)
         ENDIF
         DO k = 1, kst(n)
            READ (2,230)  kdum,  YSTAN(k,n),   USTAN(k,n),   TSTAN(k,n),
   &                      ROSTAN(k,n), MUSTAN(k,n), EVSTAN(k,n)
230         FORMAT (1X, I4, 6E12.5)
         ENDDO
      ENDDO
-----------------------------------------------------------------------------------------------------
```

nxend = 0 – More data to follow.
1 – End of data.

imode = 1 – Laminar boundary layer.
2 – Turbulent boundary layer.

mfilm(n) = 0 – No film cooling.
> 0 – Initial profile after film cooling follows immediately.

intg(n) = *x*-station number as referred to by STANDEP.

kst(n) = Number of cross-stream boundary layer points for STANDEP calculation at *x*-station n (m).

X(n) = *x*-value at station n (m).

UE(n) = Free-stream velocity at station n ($m\ s^{-1}$).

PE(n) = Static pressure at station n (Nm^{-2}).

CF(n) = Friction factor at station n.

DEL1(n) = Displacement thickness at station n (m).

DEL2(n) = Momentum thickness at station n (m).

AUX1(ifilm) = Film cooling blowing parameter.

AUX2(ifilm) = Film cooling temperature parameter.

AUX3(ifilm) = Film cooling hole diameter (m).

AUX4(ifilm) = Film cooling hole angle (degrees).

AUX5(ifilm) = Hole pitch (m).

AUX6(ifilm) = Hole skew angle (degrees).

Various profiles at *x*-station n :

YSTAN(k,n) = *y*-value at point (k,n), (mm).

USTAN(k,n) = *x*-velocity at point (k,n), ($m\ s^{-1}$).

TSTAN(k,n) = Static temperature at point (k,n), (K).

ROSTAN(k,n) = Carrier gas density at point (k,n) ($kg\ m^{-3}$).

MUSTAN(k,n) = Dynamic viscosity at point (k,n) ($kg\ m^{-1}s^{-1}$).

EVSTAN(k,n) = Eddy dynamic viscosity at point (k,n) ($kg\ m^{-1}s^{-1}$).

OUTPUT OF RESULTS

(Printed on UNIT 8)

Section 1 :

Input data and basic information which is self-explanatory.

Section 2 :

Results generated by STANDEP. The interpretation of the headings is as follows :

n	=	Number of *x*-station.
L/T	=	Laminar or turbulent boundary layer.
X mm	=	*x* value in mm.
Ye mm	=	*y* value at outer edge of STANDEP computational grid.
Ye+	=	Corresponding y_+ value.
Ue m/s	=	Free-stream velocity in m/s.
Pe bar	=	Static pressure in bar.
Te K	=	Free-stream static temperature in K.
Ti K	=	Blade surface temperature in K.
RHOe	=	Free-stream density in kg/m^3.
VISCe	=	Free-stream dynamic viscosity in kg/m s.
U* m/s	=	Friction velocity in m/s.
Cf	=	Friction factor.
D* mm	=	Displacement thickness in mm.
TH mm	=	Momentum thickness in mm.

Section 3 :

Results of vapour diffusion calculations. The interpretation of the headings is as follows:

n	=	Number of *x*-station.
L/T	=	Laminar or turbulent boundary layer.
kp	=	Number of cross-stream computational points.
GP ratio	=	Grid geometric progression ratio (should be less than 1.2).
Te (K)	=	Free-stream static temperature in K.
Ti (K)	=	Blade surface temperature in K.
Tdew (K)	=	Local dewpoint temperature in K.
Na kmol/m2s	=	Net (atomic) sodium flux in kmol/m^2s.
K kmol/m2s	=	Net (atomic) potassium flux in kmol/m^2s.

Species	=	Sodium or potassium compound.
Xe	=	Mole fraction in the free-stream.
%Na/K(e)	=	Percentage of sodium or potassium in this species in the free-stream.
Xi/Xe	=	Ratio of mole fraction at blade surface to mole fraction in free-stream.
%Na/K(i)	=	Percentage of sodium or potassium in this species at blade surface.
Xdepos	=	Mole fraction in deposit.
L/S	=	Liquid or solid deposit.
Activ	=	Activity coefficient.
Schmidt	=	Schmidt number based on free-stream conditions.
Sherwood	=	Sherwood number based on distance *x* and free-stream conditions.
Km (m/s)	=	Mass transfer coefficient in m/s (differential calculation).
kmol/m2s	=	Molar flux of species in kmol/m^{2}s, positive in away from blade surface.
NI/ND	=	Ratio of molar fluxes calculated by integral and differential methods.

When boundary layer profiles are printed, the interpretation of the headings is as follows :

k	=	Cross-stream grid point number.
Y (mm)	=	Distance from blade surface in mm.
Y+	=	$y u_* / \nu$
U/Ue	=	u / u_∞
RO/ROe	=	ρ / ρ_∞
T (K)	=	Static temperature in K.
MU/MUe	=	μ / μ_∞
EV/MU	=	Ratio of turbulent viscosity to laminar viscosity.
PSI(J)	=	Species J dimensionless concentration, PSI = $(X_j - X_{jo}) / (X_{j\infty} - X_{jo})$.

APPENDIX 1

EQUILIBRIUM OF SODIUM AND POTASSIUM SPECIES IN THE GAS PHASE

The gas components of interest are O_2, H_2O, SO_2 and HCl. It is assumed that the mole fractions of these remain fixed. The presence of the OH radical is important for the equilibrium of the Na/K species and this is controlled by the chemical reaction,

$$\frac{1}{2}\mathrm{H_2O} + \frac{1}{4}\mathrm{O_2} = \mathrm{OH}$$

which is assumed to be at equilibrium everywhere (with equilibrium constant K_{p0}). If p is the mixture pressure and X_i is the mole fraction of component i,

$$X_{\mathrm{OH}} = K_{p0} X_{\mathrm{H2O}}^{1/2} X_{\mathrm{O2}}^{1/4} p^{-1/4} \tag{A1.1}$$

Consider now the equilibrium of the sodium species (the analysis for potassium being identical in all respects). The important species defining the composition are assumed to be Na_2SO_4, NaCl, NaOH and NaO_2. The relevant chemical reactions are,

$$\mathrm{NaO_2} + \mathrm{OH} = \mathrm{NaOH} + \mathrm{O_2} \qquad (K_p = K_{p1})$$

$$2\,\mathrm{NaO_2} + \mathrm{SO_2} = \mathrm{Na_2SO_4} + \mathrm{O_2} \qquad (K_p = K_{p2})$$

$$2\,\mathrm{NaCl} + \mathrm{SO_2} + \mathrm{H_2O} + \frac{1}{2}\mathrm{O_2} = \mathrm{Na_2SO_4} + 2\,\mathrm{HCl} \qquad (K_p = K_{p3})$$

At combustor outlet, it is assumed that these reactions are at equilibrium. The following equations can then be derived relating the mole fractions of the various sodium species,

$$X_{\mathrm{NaOH}} = A X_{\mathrm{NaO2}} \qquad A = K_{p1} X_{\mathrm{OH}} X_{\mathrm{O2}}^{-1} \tag{A1.2a}$$

$$X_{\mathrm{NaSu}} = B X_{\mathrm{NaO2}}^{2} \qquad B = K_{p2} X_{\mathrm{SO2}} X_{\mathrm{O2}}^{-1} p \tag{A1.2b}$$

$$X_{\mathrm{NaCl}} = C X_{\mathrm{NaO2}} \qquad C = K_{p2}^{1/2} K_{p3}^{-1/2} X_{\mathrm{HCl}} X_{\mathrm{H2O}}^{-1/2} X_{\mathrm{O2}}^{-3/4} p^{-1/4} \tag{A1.2c}$$

where NaSu stands for Na_2SO_4. For fixed gas mole fractions, the coefficients A, B and C depend only on the mixture pressure p and the temperature (through the equilibrium constants). The total mole fraction of atomic sodium X_{Na} is specified input data and is related to the mole fractions of the sodium species by the relationship,

$$X_{\mathrm{Na}} = 2X_{\mathrm{NaSu}} + X_{\mathrm{NaCl}} + X_{\mathrm{NaOH}} + X_{\mathrm{NaO2}} = \textit{constant} \tag{A1.3}$$

Eliminating the mole fractions of Na_2SO_4, NaCl and NaOH gives the quadratic equation,

$$2B\,X_{\mathrm{NaO2}}^{2} + (1+A+C)\,X_{\mathrm{NaO2}} - X_{\mathrm{Na}} = 0 \qquad \text{(A1.4)}$$

which is easily solved for X_{NaO2}. X_{NaSu}, X_{NaOH} and X_{NaCl} then follow from equations (A1.2) above. If chlorine is absent $C = 0$ and the equation for X_{NaO2} is still quadratic. If sulphur is absent $B = 0$. The equation is then no longer quadratic but the analysis still holds.

Between the combustor outlet and the freestream in the turbine blade passage of interest, chemical reactions may occur to alter the distribution of the various sodium species. Consideration of the rates of the various reactions suggest two possibilities, both of which are available as options within the program :

1) Full equilibrium prevails in the freestream of the turbine blade passage. In this case, the analysis is identical to that described above but is carried out at the local pressure and temperature of interest.

2) The mole fraction of Na_2SO_4 is assumed frozen at the combustor outlet value but all other species maintain their equilibrium concentrations. This is considered the more realistic possibility because the formation of Na_2SO_4 requires the collision of two sodium species which, given the extremely low concentrations, must be a comparatively rare event. The analysis for frozen Na_2SO_4 is similar to the full equilibrium calculation but only two (rather than three) chemical reactions are involved. This leads to the modified equation for X_{NaO2},

$$(1+A+C)\,X_{\mathrm{NaO2}} - (X_{\mathrm{Na}} - 2X_{\mathrm{NaSu}}^{0}) = 0 \qquad \text{(A1.5)}$$

where X_{NaSu}^{0} is the mole fraction of Na_2SO_4 at combustor outlet.

The coding for the gas-phase equilibrium calculations can be found in SUBROUTINE CHEMGAS. The equilibrium constants are calculated by SUBROUTINE EQUMCONST, the data for the Gibbs free energies of formation being stored in MODULES CHEMDATA.

APPENDIX 2

SPECIES CONSERVATION EQUATION

The carrier gas is assumed to be a mixture of N_2, CO_2, H_2O and O_2, all of which behave as semi-perfect gases. The partial pressure p_i of gas component i is given by,

$$p_i = n_i \bar{R} T = \frac{\rho_i \bar{R} T}{M_i} = \rho_i R_i T \qquad \text{(A2.1)}$$

where, $\bar{R}$ = universal gas constant,
M_i = molar mass of component i,
R_i = specific gas constant of component i,
n_i = molar density of component i,
ρ_i = partial mass density of component i,
T = static temperature.

The mixture as a whole also behaves as a semi-perfect gas with pressure p given by,

$$p = n\bar{R}T = \rho RT \qquad \text{(A2.2)}$$

where $n = \Sigma n_i$ is the total molar density, $\rho = \Sigma \rho_i$ is the mixture density and $R = \Sigma m_i R_i$ is the mean specific gas constant ($m_i = \rho_i/\rho$ being the mass fraction of component i). The mean molar mass M is given by,

$$M = \Sigma X_i M_i \qquad \text{(A2.3)}$$

where, $X_i = n/n_i = p/p_i$ is the mole fraction of component i and $\Sigma X_i = 1$. The composition of the gas mixture is assumed to be constant throughout the flowfield.

Within the carrier gas there are a number of sodium and potassium species present in vapour form (Na_2SO_4, NaCl, NaOH, NaO_2, K_2SO_4, KCl, KOH and KO_2). The mole fractions of all sodium and potassium species are assumed to be extremely low so that their presence does not affect the calculation of the carrier gas properties. The values of these mole fractions at the outer edge of the boundary layer are calculated using the theory of Appendix 1 using either the full equilibrium or frozen sulphate approximation. The problem then is to compute the rate at which the sodium and potassium species diffuse through the boundary layer (which may be laminar or turbulent) and deposit in liquid or solid form on the metal surface of the blade. It is further assumed that chemical reactions within the boundary layer do not occur.

The thin shear layer approximation to the instantaneous conservation equation for

sodium or potassium species j is (neglecting thermal diffusion),

$$\frac{\partial}{\partial t}(\rho m_j) + \frac{\partial}{\partial x}(\rho u m_j) + \frac{\partial}{\partial y}(\rho v m_j) = \frac{\partial}{\partial y}\left(\rho D_j \frac{\partial m_j}{\partial y}\right) \tag{A2.4}$$

where, u = x-component of velocity,
v = y-component of velocity,
m_j = mass fraction of species j,
D_j = diffusion coefficient of species j in the carrier gas mixture.

D_j is given by the kinetic theory expression,

$$\frac{1}{D_j} = \sum_i \frac{X_i}{D_{ij}} \tag{A2.5}$$

where X_i is the mole fraction of gas component i and D_{ij} is the Chapman-Enskog first approximation to the binary diffusion coefficient of Na/K species j in gas component i,

$$D_{ij} = \frac{0.018829 T^{1.5}}{p \sigma_{ij}^2 \Omega_D} \left(\frac{M_i + M_j}{M_i M_j}\right)^{1/2} \tag{A2.6}$$

where, D_{ij} = binary diffusion coefficient ($m^2 s^{-1}$),
M_i = molar mass of gas component-i,
M_j = molar mass of Na/K species-j,
T = temperature (K),
p = mixture pressure (Nm^{-2}),
σ_{ij} = mean Lennard-Jones length parameter (Angstrom units),
Ω_D = dimensionless collision integral.

For a turbulent compressible boundary layer, time-mean and fluctuating components are introduced in the usual way. After Reynolds averaging, equation (A2.4) takes the familiar form,

$$\frac{\partial}{\partial x}(\bar{\rho}\bar{u}\bar{m}_j) + \frac{\partial}{\partial y}(\bar{\rho}\bar{v}\bar{m}_j) = \frac{\partial}{\partial y}\left[\bar{\rho}\left(D_j + D_t\right)\frac{\partial \bar{m}_j}{\partial y}\right] \tag{A2.7}$$

where the overbars represent Reynolds averaged quantities and D_t is a turbulent diffusion coefficient. D_t is related to the turbulent viscosity μ_t via the turbulent Schmidt number Sc_t,

$$Sc_t = \frac{\mu_t}{\bar{\rho} D_t} \tag{A2.8}$$

which is usually set equal to unity in the absence of more reliable experimental information. Substituting equation (A2.8) into (A2.7) gives,

$$\frac{\partial}{\partial x}(\bar{\rho}\,\bar{u}\,\bar{m}_j) + \frac{\partial}{\partial y}(\bar{\rho}\,\bar{v}\,\bar{m}_j) = \frac{\partial}{\partial y}\left[\left(\bar{\rho}\,D_j + \frac{\mu_t}{Sc_t}\right)\frac{\partial \bar{m}_j}{\partial y}\right] \tag{A2.9}$$

Because the sodium and potassium species are present only in trace amounts, the mass and mole fractions are related by,

$$\bar{m}_j = \frac{M_j}{M}\bar{X}_j \tag{A2.10}$$

and hence,

$$\frac{\partial}{\partial x}(\bar{\rho}\,\bar{u}\,\bar{X}_j) + \frac{\partial}{\partial y}(\bar{\rho}\,\bar{v}\,\bar{X}_j) = \frac{\partial}{\partial y}\left[\left(\bar{\rho}\,D_j + \frac{\mu_t}{Sc_t}\right)\frac{\partial \bar{X}_j}{\partial y}\right] \tag{A2.11}$$

For computational purposes, a scaled variable ψ_j is defined by,

$$\psi_j = \frac{\bar{X}_j - \bar{X}_{jo}}{\bar{X}_{j\infty} - \bar{X}_{jo}} \tag{A2.12}$$

where subscripts o and ∞ refer to conditions at the wall and free-stream respectively. Assuming $(\bar{X}_{j\infty} - \bar{X}_{jo})$ changes only slowly with *x*, equation (A2.11) then becomes,

$$\frac{\partial}{\partial x}(\bar{\rho}\,\bar{u}\,\psi_j) + \frac{\partial}{\partial y}(\bar{\rho}\,\bar{v}\,\psi_j) = \frac{\partial}{\partial y}\left[\left(\bar{\rho}\,D_j + \frac{\mu_t}{Sc_t}\right)\frac{\partial \psi_j}{\partial y}\right] \tag{A2.13}$$

subject to $\psi_{j\mathrm{o}} = 0$ and $\psi_{j\infty} = 1$. Hence, the variation of ψ_j across the boundary layer and the corresponding mass transfer coefficient are independent of the mole fraction difference between the wall and free-stream. This is very important because it implies that, for each species, equation (A2.13) has to be solved once, and once only, at each *x*-station. This is not the case if thermal diffusion is included, however, because it is then impossible to find a scaling variable which results in an equation which is independent of $(\bar{X}_{j\infty} - \bar{X}_{jo})$.

APPENDIX 3

GRID GENERATION

The computational grid used by the program VAPOURDEP is established by SUBROUTINE GRID.

In order to obtain accurate definition of the concentration profiles (especially when the boundary layer is turbulent) it is necessary to use an extremely fine grid spacing near the wall as turbulent wall functions are not used in the calculation procedure. If, then, the grid spacing normal to the surface remains uniform over the whole of the boundary layer, an unnecessarily large number of points is required. Accordingly, a non-uniform grid is used, the grid spacing increasing with distance from the wall as a geometric progression.

Only two parameters (specified by the user as input data) are required to establish the grid spacing normal to the wall throughout the entire flowfield. KPOINT is the total number of grid points across the boundary layer including the wall and free-stream points. For a turbulent boundary layer, KPOINT = 50 is usually satisfactory. For a laminar boundary layer, KPOINT = 30 may give good definition but there is actually no reason to restrict the number of points as the calculation is cheap in terms of CPU time even when several different Na/K species are present. The maximum number of cross-stream grid points is fixed in the program by the value of KSTZ in MODULE PARAMETERS.

The other parameter specified by the user, YWPLUS, is the value of $y_+ = y u_* / \nu$ corresponding to the first point in the boundary layer adjacent to the wall (k = 2). For a turbulent boundary layer, this point should be embedded deep in the laminar sublayer and a value of YWPLUS = 0.1 or 0.2 is often satisfactory. The same parameter YWPLUS is also used to establish the position of the point k = 2 in regions of the flow where a laminar boundary layer is present and experience shows that a value YWPLUS = 0.1 or 0.2 is also satisfactory here. Whatever value is chosen, however, it is wise to examine the computed profiles after running the program to ensure that good definition has been obtained in all regions of the flow. (Note that the value of YWPLUS should be chosen as if all Schmidt numbers were unity. Adjustment for Schmidt numbers other than unity is automatically handled by the program.)

Although the grid spacing normal to the wall used by the program VAPOURDEP will be quite different from the grid spacing used by STANDEP to generate the velocity and temperature fields, no provision has been included to alter the spacing in the x-direction parallel to the wall. The grid spacing in this direction is always precisely the same as that generated by STANDEP and boundary layer parameters computed at a given x-station by

VAPOURDEP may therefore be compared with or combined with parameters computed by STANDEP at the same location. The numbering system adopted for output by VAPOURDEP corresponds exactly to that of STANDEP, the first *x*-station being denoted by $n = 0$.

Calculation of the grid spacing normal to the wall proceeds one *x*-station at a time. With reference to Fig. 1, it is assumed that the grid at $x=x^{n-1}$ has been established and all calculations at this location have been successfully completed. The first task in establishing the grid at $x=x^{n}$ is to specify the value of $(y_+)_\infty^n$ at the free-stream point $k = K$. For $n > 0$, this is initially set equal to the value of $(y_+)_\infty^{n-1}$. However, for calculation of the initial profile at $n = 0$, a special procedure is used which acknowledges the possibility that the thickness of the concentration layer in a laminar boundary with Schmidt number less than unity may be greater than the thickness of the velocity layer.

The user-specified value of $(y_+)_2^n$ is now examined because of the possibility that the maximum Schmidt number of all the species present may be significantly greater than unity. This implies that the *concentration* sublayer in a turbulent boundary layer is much thinner than the *velocity* sublayer. Should this be the case, the value of $(y_+)_2^n$ actually used in the calculations is automatically reduced to ensure good definition near the wall.

From the known values of $(y_+)_2^n$ at $k = 2$, $(y_+)_\infty^n$ at $k = K$, and the value of *K* itself, it is now possible to calculate the ratio *R* of the geometric progression which fixes the grid spacing. The equation for *R* is,

$$(y_+)_\infty^n (R-1) \;=\; (y_+)_2^n (R^{K-1}-1)$$

and is solved iteratively by the program using a Newton-Raphson procedure. The computed value of *R* defines the rate at which the grid spacing increases away from the wall and for accurate calculations should not be greater than 1.2. The local value is printed at each *x*-station in the output listing under the heading GPRATIO. Should *R* exceed 1.2, the remedy is to specify a larger number of cross-stream grid points.

With the grid established at $x=x^{n}$, diffusion calculations for all species present are performed. The results are then examined to ensure that the computational domain extends a sufficient distance from the wall that all concentration gradients at the outer edge of the domain are very small. If this is not so, some or all of the concentration layers have thickened to such an extent that it is necessary to increase the computational domain. As a first attempt to overcome this problem, the value of $(y_+)_\infty^n$ is increased by a factor BLINC which is specified as input data by the user. Typically, setting BLINC = 1.02 allows the boundary layer thickness to increase by 2% at each *x*-station while retaining the same

number of cross-stream points and will encompass most boundary layer growth without seriously distorting the computational mesh. If, after recalculation of the concentration profiles, the convergence criteria are still not satisfied, extra points are added (one at a time) to the outer edge of the computational domain.

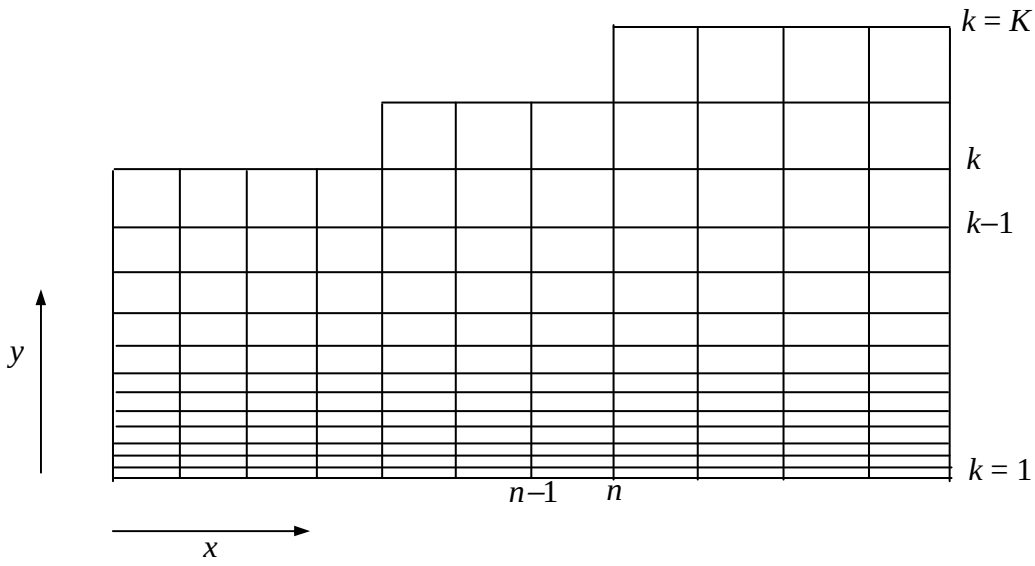

Figure 1: Non-uniform grid used by VAPOURDEP.

APPENDIX 4

FINITE VOLUME SOLUTION OF THE SPECIES CONTINUITY EQUATIONS

The integration of equation (A2.13) is effected using a finite volume technique. In the program VAPOURDEP, the calculations are performed by SUBROUTINE MATRIX which is called from PROGRAM MAIN, the main control routine.

Initially, a computational grid is established as shown in Fig. 1 (Appendix 4) by calling SUBROUTINE GRID. The procedure by which the grid is generated is described in Appendix 4 but it should be noted that the spacing need not be uniform in either co-ordinate direction to maintain formal second-order accuracy. It should also be noted that the grid spacing in the *x*-direction is identical to that used by STANDEP but that the spacing in the *y*-direction is quite different.

When, at each *x*-station, the *y*-direction grid spacing is established, the values of flow velocity, density, viscosity, etc., required by the calculation scheme are interpolated from the STANDEP grid to the VAPOURDEP grid using a variable power spline curve fitting procedure. This technique is not described here, but details can be found in Soanes, 1976. The relevant coding occurs in SUBROUTINES VPINTERP, VPCOEFF, VPMATRIX and VPSPLINE, the first routine being called directly from PROGRAM MAIN.

The coefficients of equation (A2.13) can then be computed for every grid point in the flowfield. At any stage of the calculation, values of ψ_j are known at all grid points along the line $x = x^{n-1}$ shown in Fig. 1. The problem then is to compute the values of ψ_j along the line $x = x^n$ for all nodes $y = y_k^n$. (In the cross-stream direction, there are K nodes, $k = 1$ representing the wall and $k = K$ representing the free-stream conditions respectively.)

To obtain the solution, equation (A2.13) is transformed to a first-order partial differential equation by defining a new variable $\phi = \partial\psi/\partial y$ (the subscript j having been been dropped for clarity). The finite difference representation of the defining expression is,

$$\left(\psi_k^n - \psi_{k-1}^n\right) - \frac{1}{2}\left(\phi_k^n + \phi_{k-1}^n\right)\left(y_k^n - y_{k-1}^n\right) = 0 \qquad \text{(A3.1)}$$

an equation which is valid for $2 \le k \le K$.

Equation (A2.13) is then written in finite volume form by integrating over a computational cell and applying Gauss's theorem. This gives (for $2 \le k \le K$),

$$F_{k-1/2}^{n}\left(\psi_k^n + \psi_{k-1}^n\right) - F_{k-1/2}^{n-1}\left(\psi_k^{n-1} + \psi_{k-1}^{n-1}\right) +$$
$$G_k^{n-1/2}\left(\psi_k^n + \psi_k^{n-1}\right) - G_{k-1}^{n-1/2}\left(\psi_{k-1}^n + \psi_{k-1}^{n-1}\right) +$$
$$H_k^{n-1/2}\left(\phi_k^n + \phi_k^{n-1}\right) - H_{k-1}^{n-1/2}\left(\phi_{k-1}^n + \phi_{k-1}^{n-1}\right) = 0 \qquad \text{(A3.2)}$$

The coefficients F, G and H are given by,

$$F_{k-1/2}^{n} = \frac{1}{2}\left(y_k^n - y_{k-1}^n\right)\left(\bar{\rho}_k^n \bar{u}_k^n + \bar{\rho}_{k-1}^n \bar{u}_{k-1}^n\right) \qquad (\text{for } 2 \le k \le K)$$

$$G_k^{n-1/2} = \sum_{i=2}^{k} F_{i-1/2}^{n-1} - \sum_{i=2}^{k} F_{i-1/2}^{n} \qquad (\text{for } 2 \le k \le K)$$

$$H_k^{n-1/2} = \frac{1}{2}\left(x^n - x^{n-1}\right)\left(A_k^n + A_k^{n-1}\right) \qquad (\text{for } 1 \le k \le K) \qquad \text{(A3.3)}$$

where the variable A is defined by,

$$A = -\left(\bar{\rho} D_j + \frac{\mu_t}{Sc_t}\right) \qquad \text{(A3.4)}$$

In the second of equations (A3.3), $G_k^{n-1/2}$ is only defined for $2 \le k \le K$. For k = 1, the condition of zero mass flux through the wall implies $G_1^{n-1/2} = 0$.

Equations (A3.1) and (A3.2) are written for $2 \le k \le K$, thus providing a total of (2K–2) equations for the 2K unknowns (i.e., the values of ψ_k^n and ϕ_k^n for $1 \le k \le K$). The remaining two equations are supplied by the boundary conditions at the free-stream and the vapour-liquid interface. At the free-stream,

$$\psi_K^n = 1 \qquad \text{(A3.5)}$$

and at the vapour-liquid interface,

$$\psi_1^n = 0 \qquad \text{(A3.6)}$$

The solution of the equation set proceeds by writing equation (A3.1) in the form,

$$a_{k1}\psi_{k-1}^n + a_{k2}\phi_{k-1}^n + a_{k3}\psi_k^n + a_{k4}\phi_k^n = a_{k5} \qquad \text{(A3.7)}$$

where,

$$a_{k1} = 1, \quad a_{k2} = \frac{1}{2}\left(y_k^n - y_{k-1}^n\right), \quad a_{k3} = -1, \quad a_{k4} = \frac{1}{2}\left(y_k^n - y_{k-1}^n\right), \quad a_{k5} = 0 \qquad \text{(A3.8)}$$

Likewise, equation (A3.2) can be written,

$$b_{k1}\psi_{k-1}^{n} \;+\; b_{k2}\phi_{k-1}^{n} \;+\; b_{k3}\psi_{k}^{n} \;+\; b_{k4}\phi_{k}^{n} \;=\; b_{k5} \tag{A3.9}$$

where,

$$\begin{aligned}
b_{k1} &= F_{k-1/2}^{n} - G_{k-1}^{n-1/2} \\
b_{k2} &= -H_{k-1}^{n-1/2} \\
b_{k3} &= F_{k-1/2}^{n} + G_{k}^{n-1/2} \\
b_{k4} &= H_{k}^{n-1/2} \\
b_{k5} &= \left(F_{k-1/2}^{n-1} + G_{k-1}^{n-1/2}\right)\psi_{k-1}^{n-1} + H_{k-1}^{n-1/2}\phi_{k-1}^{n-1} + \\
&\quad \left(F_{k-1/2}^{n-1} + G_{k}^{n-1/2}\right)\psi_{k}^{n-1} - H_{k}^{n-1/2}\phi_{k}^{n-1}
\end{aligned} \tag{A3.10}$$

The finite volume equations (A3.7) and (A3.9), together with the boundary conditions, equations (A3.5) and (A3.6), can then be written in matrix-vector form,

$$\begin{bmatrix}
1 & 0 & 0 & & & & & & & \\
a_{21} & a_{22} & a_{23} & a_{24} & & & & & & \\
b_{21} & b_{22} & b_{23} & b_{24} & & & & & & \\
 & & a_{31} & a_{32} & a_{33} & a_{34} & & & & \\
 & & b_{31} & b_{32} & b_{33} & b_{34} & & & & \\
 & & & & \cdots & \cdots & \cdots & \cdots & & \\
 & & & & \cdots & \cdots & \cdots & \cdots & & \\
 & & & & & & a_{k1} & a_{k2} & a_{k3} & a_{k4} \\
 & & & & & & b_{k1} & b_{k2} & b_{k3} & b_{k4} \\
 & & & & & & & & 1 & 0
\end{bmatrix}
\begin{bmatrix}
\psi_{1n} \\ \phi_{1n} \\ \psi_{2n} \\ \phi_{2n} \\ \cdots \\ \cdots \\ \cdots \\ \cdots \\ \psi_{kn} \\ \phi_{kn}
\end{bmatrix}
=
\begin{bmatrix}
0 \\ a_{25} \\ b_{25} \\ a_{35} \\ b_{35} \\ \cdots \\ \cdots \\ a_{k5} \\ b_{k5} \\ 1
\end{bmatrix} \tag{A3.11}$$

Equation (A3.11) is linear in the ψ_k^n and ϕ_k^n and is easily solved by a single pass of Gaussian elimination. The relevant coding can be found in SUBROUTINE MATRIX.

APPENDIX 5

SPECIFICATION OF THE INITIAL CONCENTRATION PROFILES

The initial dimensionless concentration profiles are computed automatically by the program VAPOURDEP. Four possibilities are available to the user as follows :

1) Self-similar profile corresponding to a laminar boundary layer on a flat plate with zero pressure gradient.
2) Self-similar profile corresponding to a laminar BL near a stagnation point.
3) Profile corresponding to a turbulent BL on a flat plate with zero pressure gradient.
4) Profile corresponding to a turbulent BL near a stagnation point.

Profiles 1 and 3 are chosen by setting the input variable IPROFIL = 0. Profiles 2 and 4 are chosen by setting IPROFIL = 1. The laminar and turbulent options are automatically specified by the output data generated by STANDEP.

All the profiles are generated by applying the same transformation to the species conservation equation (A2.13). A streamfunction Ψ, defined by,

$$\overline{\rho}\,\overline{u} = \frac{\partial \Psi}{\partial y} \qquad\qquad \overline{\rho}\,\overline{v} = -\frac{\partial \Psi}{\partial x} \tag{A5.1}$$

is given by,

$$\Psi = (\rho_\infty u_\infty x)^n \mu_\infty^{1-n} f(x,\eta) \tag{A5.2}$$

where,

$$d\eta = \left(\frac{\rho_\infty u_\infty}{\mu_\infty}\right)^n \left(\frac{\overline{\rho}}{\rho_\infty}\right) x^{n-1}\, dy \tag{A5.3}$$

For n = 0.5, it can be seen that the equations reduce to the compressible Falkner-Skan transformation. Applying the transformation to equation (A2.13) results in,

$$\frac{\partial}{\partial \eta}\left[\left(\frac{\rho\mu}{\rho_\infty \mu_\infty}\right)\left(\frac{1}{Sc_j}\right)\left(1+\frac{\mu_t Sc_t}{\mu\, Sc_j}\right)\frac{\partial \psi_j}{\partial \eta}\right] +$$

$$n\left[1+\frac{d(\ell n\, u_\infty)}{d(\ell n\, x)}+\frac{d(\ell n\, \rho_\infty)}{d(\ell n\, x)}-\left(\frac{n-1}{n}\right)\frac{d(\ell n\, \mu_\infty)}{d(\ell n\, x)}\right] f\,\frac{\partial \psi_j}{\partial \eta} = x\left(\frac{\partial f}{\partial \eta}\frac{\partial \psi_j}{\partial x}-\frac{\partial f}{\partial x}\frac{\partial \psi}{\partial \eta}\right) \tag{A5.4}$$

where the overbars have been dropped for convenience. Defining,

$$M = \frac{d(\ell n\, u_\infty)}{d(\ell n\, x)} \tag{A5.5}$$

it can be seen that $M = 0$ corresponds to flow over a flat plate with zero pressure gradient and $M = 1$ to flow near a stagnation point (where u_∞ varies directly with x). For $M = 0$, it automatically follows that,

$$\frac{d(\ell n\, \rho_\infty)}{d(\ell n\, x)} = \frac{d(\ell n\, \mu_\infty)}{d(\ell n\, x)} = 0 \tag{A5.6}$$

Near a stagnation point, the velocity is low and so, for $M = 1$, equations (A5.6) also apply.

The laminar profiles are obtained by setting $(\partial/\partial x)_\eta = 0$, $\mu_t = 0$ and $n = 0.5$ in equation (A5.4) to give,

$$\frac{\partial}{\partial \eta}\left[\left(\frac{\rho\mu}{\rho_\infty \mu_\infty}\right)\left(\frac{1}{Sc_j}\right)\frac{\partial \psi_j}{\partial \eta}\right] + (1+M)\frac{f}{2}\frac{\partial \psi_j}{\partial \eta} = 0 \tag{A5.7}$$

Transforming back to the (x,y) co-ordinate system gives,

$$\frac{\partial}{\partial y}\left[\rho D_j \frac{\partial \psi_j}{\partial y}\right] + (1+M)\frac{F}{2}\frac{\partial \psi_j}{\partial y} = 0 \tag{A5.8}$$

where $F = (\rho_\infty u_\infty \mu_\infty / x)^{0.5} f$ and

$$\rho u = x\frac{\partial F}{\partial y} \tag{A5.9}$$

F is easily calculated by numerical integration of equation (A5.9) subject to the boundary condition $F = 0$ at $y = 0$. The concentration profile is then obtained by numerical solution of equation (A5.8). The procedure used parallels that employed for the general solution of equation (A2.13) and only necessitates the introduction of a few extra lines of code when setting up the matrix coefficients in SUBROUTINE MATRIX.

Quite a good approximation for the initial turbulent concentration profiles can be obtained by suppressing the x-dependence in equation (A5.4) and adjusting the value of n to give the required mass transfer coefficient corresponding to $M = 0$ or $M = 1$. Performing the manipulation and transforming back to the (x,y) co-ordinate system gives,

$$\frac{\partial}{\partial y}\left[\left(\overline{\rho} D_j + \frac{\mu_t}{Sc_t}\right)\frac{\partial \psi_j}{\partial y}\right] + n(1+M)F\frac{\partial \psi_j}{\partial y} = 0 \tag{A5.10}$$

where $F = (\rho_\infty u_\infty)^n (\mu_\infty / x)^{1-n} f$ and

$$\bar{\rho}\,\bar{u} = x\frac{\partial F}{\partial y} \tag{A5.11}$$

Once the value of the parameter *n* has been chosen, the method of integration of equations (A5.10) and (A5.11) is identical to that for the laminar cases. (Note that the variation of μ_t is obtained from the output of the STANDEP calculation.) For a flat plate with zero pressure gradient, a value of $n = 0.62$ is suggested on theoretical grounds but, in practice, $n = 0.7–0.8$ (depending on the Reynolds number) gives superior results and is therefore recommended. Probably a similar value of *n* will also give a suitable starting profile near a stagnation point but there is no information in the literature to justify this hypothesis.

The generation of initial concentration profiles following a film cooling location is performed exactly as described above, the flat plate zero pressure gradient and turbulent boundary layer options being specified automatically by VAPOURDEP. The parameter *n* can be adjusted to generate any value of the Sherwood number following gas injection which is considered realistic. Currently, no information is available in the literature to serve as a guide and it is therefore suggested that values of $n = 0.7–0.8$ should be used at all film cooling locations until further data is reported. However, in order to allow freedom of choice for experimentation, the parameter *n* can be specified by the user in the input data, where it is denoted TURBN.

APPENDIX 6

CALCULATION OF MASS TRANSFER COEFFICIENTS

The mass transfer coefficient k_j of Na/K species j is defined in terms of the mass flux at the blade surface by the relationship,

$$k_j \rho_\infty (m_{jo} - m_{j\infty}) = -\rho_o D_{jo} \left(\frac{\partial m_j}{\partial y} \right)_o \tag{A6.1}$$

where m_j is the mass fraction of species j, ρ is the density of the carrier gas and subscripts o and ∞ represent conditions at the surface and free-stream respectively. An alternative definition can be made in terms of the molar flux by the defining relationship,

$$k_j n_\infty (X_{jo} - X_{j\infty}) = -n_o D_{jo} \left(\frac{\partial X_j}{\partial y} \right)_o \tag{A6.2}$$

where X_j is the mole fraction of species j and n is the total molar density of carrier gas. The dimensions of k_j are LT^{-1} and its numerical value in equations (A6.1) and (A6.2) is the same. The dimensionless Sherwood number (based on distance x) is defined by,

$$(Sh_j)_x = \frac{k_j x}{D_{j\infty}} \tag{A6.3}$$

Two methods are used by VAPOURDEP to calculate the value of k_j. The first involves the direct evaluation of the RHS of equation (37) by calculating the gradient of the mole fraction X_j at the wall from the computed ψ_j profile. This is referred to as the differential method and values of k_j obtained thus are listed under the heading Km(m/s) in the program output. The second method utilises the boundary layer integral relation,

$$k_j n_\infty (X_{jo} - X_{j\infty}) = \frac{d}{dx} \left[n_\infty u_\infty (X_{jo} - X_{j\infty}) \delta_{cj} \right] \tag{A6.4}$$

where δ_{cj} is a concentration thickness defined by,

$$\delta_{cj} = \int_0^\infty \frac{\bar{\rho}\bar{u}}{\rho_\infty u_\infty} \left(\frac{X_{j\infty} - X'_j}{X_{j\infty} - X_{jo}} \right) dy \tag{A6.5}$$

Usually, the values of k_j calculated from equations (A6.2) and (A6.4) agree to within 1%. Their ratio is listed under the heading NI/ND in the program output and the deviation from unity gives some indication of the accuracy of the numerical method.

APPENDIX 7

EQUILIBRIUM AT THE GAS-DEPOSIT INTERFACE

At the blade surface, the program implements a special thermo-chemical boundary condition which assumes the existence of a liquid or solid deposit on the metal. The underlying assumptions and the theory is complex and only a brief outline is provided here. The main assumption is that the sodium and potassium species in the gas phase directly in contact with the deposit are assumed to be in thermodynamic equilibrium with each other and also with the components of the deposit. It is further assumed that the deposit is composed of Na_2SO_4 and K_2SO_4 only. At present, the user must choose, via the input data, whether the deposit is to be considered liquid or solid.

Calculation of the equilibrium composition in the gas phase is straightforward once the mole fractions of Na_2SO_4 and K_2SO_4 in the deposit are known. Denoting mole fractions in the gas phase by X and in the liquid or solid deposit by Y, the application of Raoult's law with modifications for non-ideal behaviour and ionic dissociation gives,

$$X_{\mathrm{NaSu}} = \gamma_{\mathrm{NaSu}} \left(\frac{p^*_{\mathrm{NaSu}}(T)}{p} \right) Y^2_{\mathrm{NaSu}} \qquad \text{(A7.1a)}$$

$$X_{\mathrm{KSu}} = \gamma_{\mathrm{KSu}} \left(\frac{p^*_{\mathrm{KSu}}(T)}{p} \right) Y^2_{\mathrm{KSu}} \qquad \text{(A7.1b)}$$

$$Y_{\mathrm{NaSu}} + Y_{\mathrm{KSu}} = 1 \qquad \text{(A7.2)}$$

where NaSu and KSu stand for Na_2SO_4 and K_2SO_4 respectively, γ_{NaSu} and γ_{KSu} are activity coefficients, p^*_{NaSu} and p^*_{KSu} are the saturated vapour pressures at the interface temperature T (over pure liquid or solid as appropriate) and p is the mixture pressure. Y_{NaSu} and Y_{KSu} appear as squared terms because it is assumed that the Na_2SO_4 and K_2SO_4 are fully ionised in the deposit, each contributing two cations per undissociated molecule.

The activity coefficients are obtained by assuming an empirical expression for the non-ideal or *excess* Gibbs function for a mixture of Na_2SO_4 and K_2SO_4. Manipulation of this expression then gives the following equations for the activity coefficients,

$$\overline{R}T\,\ell n(\gamma_{\mathrm{NaSu}}) = (1-Y_{\mathrm{NaSu}})^2 \left[A_0 + (4Y_{\mathrm{NaSu}} - 1)A_1 \right] \qquad \text{(A7.3a)}$$

$$\overline{R}T\,\ell n(\gamma_{\mathrm{KSu}}) = (1-Y_{\mathrm{KSu}})^2 \left[A_0 + (1-4Y_{\mathrm{KSu}})A_1 \right] \qquad \text{(A7.3a)}$$

where A_0 and A_1 are constants (different for liquid and solid solutions).

The equilibrium between the vapour species is represented by equations (A1.2), evaluated at the interface rather than the free-stream temperature. Thus, for the sodium species,

$$X_{\mathrm{NaOH}} = A X_{\mathrm{NaO2}} \qquad A = K_{p1} X_{\mathrm{OH}} X_{\mathrm{O2}}^{-1} \tag{A7.3a}$$

$$X_{\mathrm{NaSu}} = B X_{\mathrm{NaO2}}^{2} \qquad B = K_{p2} X_{\mathrm{SO2}} X_{\mathrm{O2}}^{-1} p \tag{A7.3b}$$

$$X_{\mathrm{NaCl}} = C X_{\mathrm{NaO2}} \qquad C = K_{p2}^{1/2} K_{p3}^{-1/2} X_{\mathrm{HCl}} X_{\mathrm{H2O}}^{-1/2} X_{\mathrm{O2}}^{-3/4} p^{-1/4} \tag{A7.3c}$$

For an assumed values of Y_{NaSu} and a given surface temperature, X_{NaSu} can be calculated from equation (A7.1a). X_{NaO2} can then be obtained from equation (A7.3b), X_{NaOH} from equation (A7.3a) and X_{NaCl} from equation (A7.3c). A similar procedure gives the mole fractions for the potassium species. The coding for these calculations can be found in SUBROUTINE THERMOCHEM.

Having found the gas-phase composition at the interface for an assumed deposit composition, the molar fluxes of the various species through the boundary layer can be calculated. Thus, the molar flux of species *j* from the surface is given by,

$$J_j = k_j n_\infty (X_{jo} - X_{j\infty}) \tag{A7.4}$$

where k_j is the mass transfer coefficient, n_∞ is the free-stream molar density ($p/\overline{R}T$), and $X_{j\infty}$ and $X_{j\mathrm{o}}$ are the mole fractions in the free-stream and at the interface respectively.

The total molar fluxes of atomic sodium and potassium are now given by,

$$J_{\mathrm{Na}} = 2J_{\mathrm{NaSu}} + J_{\mathrm{NaCl}} + J_{\mathrm{NaOH}} + J_{\mathrm{NaO2}} \tag{A7.5a}$$

$$J_{\mathrm{K}} = 2J_{\mathrm{KSu}} + J_{\mathrm{KCl}} + J_{\mathrm{KOH}} + J_{\mathrm{KO2}} \tag{A7.5b}$$

For steady-state deposition (or evaporation of an existing deposit), the ratio of these fluxes must equal the molar ratio of atomic sodium and potassium in the deposit. Thus,

$$\frac{J_{\mathrm{Na}}}{J_{\mathrm{K}}} = \frac{Y_{\mathrm{NaSu}}}{Y_{\mathrm{KSu}}} \tag{A7.6}$$

The program therefore iterates on the value of Y_{NaSu} until equation (A7.6) is satisfied, thus establishing the composition of the deposit. The iteration method used is a numerical scheme known as the secant method. The coding can be found in SUBROUTINE INTERFACE.

The dewpoint temperature is defined as the surface temperature above which a stable liquid or solid deposit cannot form (*i.e.*, any deposit present will evaporate). At the dewpoint

temperature $J_{Na} \rightarrow 0$ and $J_K \rightarrow 0$ independently while still satisfying the requirement of equation (A7.6). By iterating simultaneously on the surface temperature and the mole fraction of Na_2SO_4 in the deposit (while assuming the local free-stream mole fractions and the mass transfer coefficients remain unaltered), it is possible to calculate the dewpoint temperature at each *x*-station. The iteration is carried out using a two-variable Newton-Raphson procedure with numerical evaluation of the four derivatives required by the scheme. The coding can be found in SUBROUTINE DEWPOINT.

APPENDIX 8

THERMODYNAMIC PROPERTIES

Routines for calculating the following thermodynamic and transport properties are included in the program :

SUBROUTINE EQUMCONST
Calculation of equilibrium constants for all chemical reactions. Gibbs free energies of formation are stored in MODULE CHEMDATA.

SUBROUTINE DIFFCOEFF
Calculation of diffusion coefficients of Na/K species in a given carrier gas mixture using the Chapman-Enskog first approximation assuming a Lennard-Jones interaction potential.

SUBROUTINE SATVAP
Calculation of saturated vapour pressures of pure salt vapour over both liquid and solid phases from empirical correlations.

All data for these routines are stored in MODULE CHEMDATA.

REFERENCES

Crawford, M.E. and Kays, W.M., 1976, "STAN5 - A program for numerical computation of two-dimensional internal and external boundary layer flows", NASA report no. CR-2742.

Soanes Jnr., R.W., 1976, "VP - splines, an extension of twice differentiable interpolation", Proc. 1976 Army Numerical Analysis and Computers Conference, ARO report 76-3, U.S. Army Res. Office, P.O. Box 12211, Res. Triangle Park, N.C., pp. 141 - 152.